Temporal and spatial characteristics of drought, future changes and possible drivers over Upper Awash Basin, Ethiopia, using SPI and SPEI

Haftu Brhane Gebremichael[1] · Gelana Amente Raba[1] · Kassahun Ture Beketie[2] · Gudina Legese Feyisa[2]

Abstract

Drought is a global problem that affects particularly agricultural and water resources. The spatiotemporal drought characteristics and their possible drivers over Upper Awash Basin (UAB) were assessed in magnitude, duration, frequency, and intensity. Gridded data and a statistical downscaling model (SDSM) were used for historical projection. The Standardized Precipitation Index (SPI) and Standardized Evapotranspiration Index (SPEI) at 4- and 12-month timescales were used to compute the drought. The SPI 4-and 12-months indicate 1984, 1987, 2002, 2015, and 2016 years of dominant drought. Persistent dry events were observed in the west, northwestern, and some eastern parts of the study area in Representative Concentration Pathways (RCP) 4.5 and 8.5 scenarios. Trend analysis of seasonal shows that a statistically significant ($P < 0.05$) increasing trend during the main cropping seasons and annual drought events were detected in almost all basin parts. Near future projections in the two (RCP4.5 and RCP8.5) scenarios exhibited the continuation of drought up to 2030s and mid-2040s extreme and severe dryness, respectively. The seasonal and annual analysis projection indicates a decrease in dry events from 2050 onwards. The detected periodicity of dryness/wetness agreed with the negative/positive phase of SOI/ENSO (Nino3.4) during Belg and the positive/negative phase during Kiremt and annual (SPI4/SPEI4). The possible driving forces of these drought events were land use/cover changes such as land degradation and urbanization. Global indices IOD, SOI, and ENSO (NINO3.4) are drivers that caused the seasonal droughts. These findings are useful for better preparedness priorities that suggest developing basin-wide targeted interventions.

Keywords Drought · Possible drivers · SPEI · SPI · Statistical downscaling model · Upper Awash Basin

---

✉ Haftu Brhane Gebremichael
  haftuberhane@gmail.com

Extended author information available on the last page of the article

1 Introduction

Climate change is a global and regional problem and has a profound impact on low-income drought-stricken countries (Farooqi et al., 2020). Drought is an insidious natural hazard that is a common part of the climate in almost all regions (Wilhite, 2003). Globally, droughts account for about one-fifth of the damage caused by natural disasters (Srinivasarao et al., 2020). It is a serious natural disaster that affects more people than any other natural disaster (Bobrowsky, 2013). It is also the main cause of severe economic losses in agricultural production, which ultimately affects the supply of food for people (Farooqi et al., 2020; Shi & Hussain, 2020). When social, economic, or environmental effects become apparent, it is commonly referred to as a natural disaster (Bobrowsky, 2013; Wilhite, 2000). In most populous regions of the world, drought has far-reaching social and economic consequences that make it difficult to manage (Below et al., 2007).

Drought is considered a long-term average state of equilibrium between rainfall and evapotranspiration (Wilhite, 2000). Although there are many definitions of drought, there is no global definition (Tate & Gustard, 2000; Wilhite, 2000). Each discipline included different physical, biological, and/or socioeconomic factors in drought definition (Wilhite, 2000). Drought is normally defined as a "prolonged absence or marked deficiency of precipitation," a "deficiency of precipitation that consequences in a water deficiency for some activity or some group," or a "period of unusually dry weather adequately prolonged for the lack of precipitation to cause a serious hydrological imbalance" (Trenberth et al., 2014). This last definition Trenberth et al. (2014) was used in this study. It must be known that the importance of drought lies in its influences or application-specific and reflects specific regional climatic characteristics for use in operational mode by decision-makers (Wilhite, 2000). Droughts can generally be divided into meteorological, agricultural, hydrological, and socioeconomic droughts (Ho et al., 2012; Wilhite, 2000; Wilhite & Glantz, 1985). In this study, the focus is on the characterization of agricultural, climatology, and hydrological drought impact. They differ in three essential characteristics: intensity, duration, and spatial coverage (Bobrowsky, 2013; Mbiriri et al., 2019; Report, 2006; Wilhite, 2003). Therefore, they can be considered dangerous multidimensional phenomena (Tsakiris & Vangelis, 2005). The severity of a drought depends not only on the intensity, duration, and geographic extent of a particular drought occurrence but also on the water supply demands made by human activities and vegetation in an area (Wilhite, 2000).

Among the drought, causes are crop losses, migration, malnutrition, poverty, and food insecurity. Drought is also linked to environmental degradation in terms of desertification and aridity of the land (Srinivasarao et al., 2020). They occur in all climatic zones, regardless of the region's normal rainfall rates and trends Slette et al. (2019), and their beginnings and cessation are difficult to know, unlike other natural disasters, making them highly unpredictable (Park et al., 2017). Climate variability and frequent droughts have caused considerable strain on water resources in most world regions, with the arid and semi-arid parts being the most pretentious (Bhaga et al., 2020). Drought stress leads to water scarcity conditions that negatively affect physiological and biochemical processes that ultimately threaten crop production (Kaushal, 2019). Droughts can also seriously negatively impact the water quality required for irrigated agriculture (Peña-Guerrero et al., 2020). Over the last few decades, repeated drought and famine in sub-Saharan Africa have had a devastating effect on the economic and social situation already characterized by serious difficulties (Tadesse et al., 2008).

Investigating and quantifying drought events can be essential to guide mitigation and adaptation options to address climate change (Wang et al., 2014). A drought assessment study is important for areas that depend on groundwater and rainfed agriculture (Ahmed et al., 2016). Africa's agriculture sector is affected by drought and needs characterization of drought events in terms of duration, severity, and intensity for proactive policy and planning (Fanadzo et al., 2021; Meza et al., 2021; Yacoub & Tayfur, 2020). For example, of all the natural disasters, droughts account for only 8% of the world's phenomenon. Nonetheless, it accounts for 25% in Africa between 1960 and 2006 (Gautam, 2006). Food security is extremely sensitive to climate risks mainly in Ethiopia and the horn of Africa. The recent climate-linked events such as the 2011 food security disasters in the Horn of Africa have emphasized the impact of droughts and floods on food production, agricultural activities, etc. (Getaneh et al., 2022). During the 1980s, a drought killed more than half a million people in Africa (Dai, 2011). In Sub-Saharan Africa, crop production and food security are at high risk of drought, where the effects are temporal and long-lasting (Shiferaw et al., 2014). According to the report of Haile et al. (2020), drought changes over East Africa follow the "dry gets drier and wet gets wetter" paradigm. It needs more attention to identify the causes to minimize the impacts and resilience methods (Yang et al., 2019). The study by Shepherd et al. (2013) on the hazard indicator shows the greatest change over time in East Africa, with increasing high temperature having an impact on the future hazard over the highlands of Ethiopia. According to Ghebrezgabher et al. (2016), climate change has been a serious and active environmental issue in the Horn of Africa for the previous eight and a half decades. Therefore, it is vital to investigate climate change's impact on future East African drought conditions for society and policymakers for effective drought mitigation, adaptation, and future drought risks (Haile et al., 2020).

The analysis of the future projection spatial–temporal evolution of drought is very important as the past drought occurrence in the basin is alarming. Therefore, to cope early with the drought in the study area, it is vital to quantify the spatiotemporal evolution of dryness to develop adaptation and mitigation strategies. Droughts negatively impact agricultural production and water resources; thus, drought projections are vigorous for developing future drought mitigation approaches (Yao et al., 2020). Based on Ayugi et al. (2021), identifying possible drought hotspots over East Africa, thus enabling timely preparation for such events, is vital. Therefore, it needs basin-wise characterization of drought in the future. Ethiopia is among the countries in East Africa that experiences extreme climate events, both drought and flood. It is also one of the countries in the region facing climate-related risks attributed to climate change and its unpredictability (Burnett, 2013; Gezie, 2019). Every two decades found increasing drought trends in spatial and temporal drought patterns from time to time (Haile et al., 2022). Ethiopia has been experiencing at least two severe droughts (Bezu, 2020). Some studies in Ethiopia assume that these droughts are partly connected to global phenomena. Scholars like Funk (2012) and Dubache et al. (2019) studied the influence of global climate change on Ethiopia's frequent drought occurrences. Based on the report by Workie and Debella (2018), the climate of Ethiopia is mostly influenced by the seasonal migration of the Inter-Tropical Converging Zone (ITCZ), the complex topography, and the teleconnection of global atmospheric circulation. The report by Funk (2012) found that most drought years in Ethiopia, such as 2015, were linked with the El Niño–southern oscillation (ENSO). However, it is still necessary to know whether this is true and whether there are other atmospheric and oceanic phenomena involved.

To understand the impact of climate change on drought, mapping drought-vulnerable areas along with socioeconomic data are important (Senamaw et al., 2021). For this purpose, drought characterization is important. From among the drought indices,

SPI and SPEI are well-tested indices in the characterization of drought in East Africa as well as in different parts of Ethiopia (Haile et al., 2020, 2022; Mekonen et al., 2020; Okal et al., 2020; Polong et al., 2019; Senamaw et al., 2021). SPI has been used in previous research works to study the drought characteristic in the Awash River basin (Adane et al., 2020; Belayneh et al., 2016; Gebreyesus, 2020). However, it is vital to explore drought in Ethiopia utilizing different indices of climatic variables such as evapotranspiration and soil water content (Mekonen et al., 2020). The use of SPEI with SPI could enable researchers to see spatial distribution and the magnitude of the severity of drought.

As the main water source of Awash River is the upper basin, it is better to characterize the past and future drought events in terms of seasonal, duration, severity, and intensity. Up to now, not much attention has been paid to the basin in this regard. We consider that this study that focuses on the basin's spatial and temporal drought patterns and future projections is important in crop production and water supplies in the basin. The Upper Awash basin is one of the most important basins in crop production and water supply in the country. What is not yet clear in the basin is drought in terms of duration, severity, intensity, and frequency of drought occurrence. To understand the possible future drought conditions in the upper Awash basin, it is better to characterize historical and future climate change on agricultural and hydrological drought events. As the main water source of the Awash River is the upper basin, understanding the link between climate change and drought events will help policymakers' future. Therefore, the objective of this study was first to understand and evaluate the past and future drought severity levels and characterizes drought in terms of magnitude, duration, frequency, and intensity using a statistical downscaling model under RCP 4.5 and 8.5 at different spatiotemporal scales using both SPI and SPEI indices in the Upper Awash Basin (Ethiopia). Second, to characterize the trends and future seasonal drought of the two cropping seasons using Ethiopia's seasonal classification as Belg (February to May) and Kiremt (June to September) and to check whether there are links with the possible global climate forcing. Therefore, this study helps stakeholders, policy, and decision-makers with effective drought monitoring, local-scale planning, and the development of context-specific drought preventive measures and early warning systems.

2 Data and methodology

2.1 Description of the UAB

The drought characterization was conducted in the Upper Awash Basin between 8°6′36″ to 9°17′56.4″ North and 37°57′25.2″ to 39°13′12″ East (Gebremichael et al., 2022). The basin is located in the central part of Ethiopia, and its elevation ranges from 1500 m above sea level at the break of the Great African Rift Valley to 3000 m on the plateau. The location of the stations and study area are shown in Fig. 1. Geographic coordinates and elevation of the stations are given in Table 1.

The predominant (93.2%) land use/cover (LULC) of the Upper Awash Basin consists of cultivated agricultural land, and the rest, 6.8%, is covered by others (Kurkura, 2011). Halcrow (2006) underlines soil erosion and land degradation as the major issues in the Upper Awash River Basin. According to Kerim et al. (2016), the landscape of the basin comprises highlands, escarpments, and rift valleys. The key physiographic topographies of the Awash
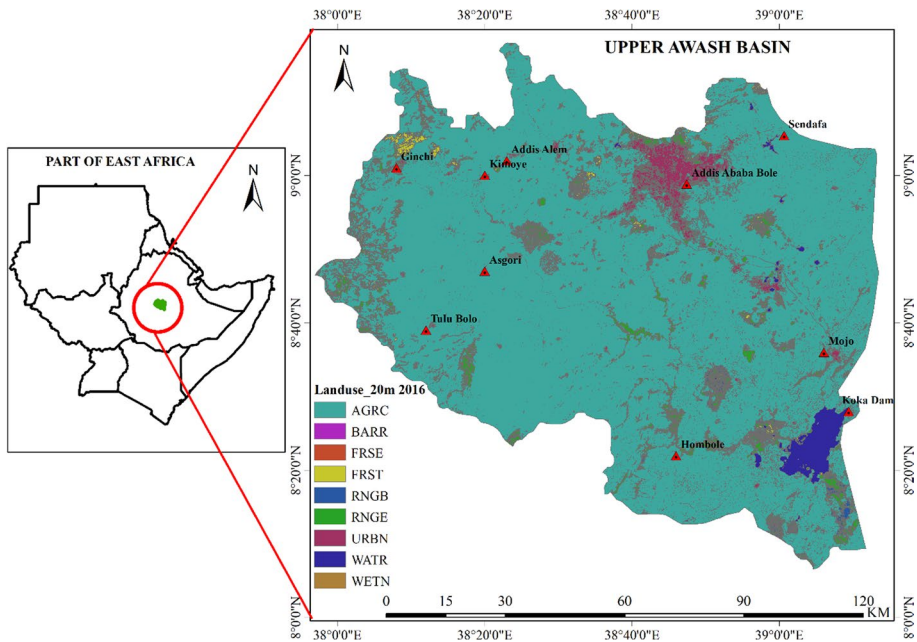
Fig. 1 Map of the upper Awash basin with the locations of Meteorological stations: AGRC = Agricultural Land; BARR = Barren; FRSE = Forest-Evergreen; FRST = Forest-mixed; RNGB = Range-Brush; RNGE-Range-Grasses; URBN = Residential; WATR = Water and WETN = Wetlands-mixed

Table 1 Geographical descriptions of meteorological stations (Gebremichael et al., 2022)

Stations	Geographical coordinates		Elevation (m) m.e. a.s.l
	Longitude (°E)	Latitude (°N)	
Addis Ababa Bole	38.79	8.98	2354
Addis Alem	38.383	9.033	2372
Asgori	38.333	8.783	2072
Koka Dam	39.156	8.466	1618
Ginchi	38.133	9.0167	2132
Hombole	38.766	8.366	1743
Kimoye	38.333	9.0	2150
Mojo	39.1	8.6	1761
Sendafa	39.01	9.09	2560
Tulu Bolo	38.2	8.65	2190

m e a.s.l = mean elevation above sea level

River Basin are the Ethiopian Rift valley and the plateau that expands to the north into the Afar Triangle. The geography of the Ethiopian Plateau is commonly flat, with elevations ranging from 2000 to 3000 m (Azazh, 2008).

2.2 Data sources

The station data used in this study from 1983 to 2016 (> 30 years) are the combined dataset, which consists of the daily observed station data of the National Meteorological Agency (NMA) and satellite data. The combined dataset consists of the observed station data from the national network managed by the NMA and the satellite data (rainfall and temperature) estimations from the European Organization for the Exploitation of Meteorological Satellites (EUMETSAT) and US National Aeronautics and Space Administration (NASA) (Dinku et al., 2014, 2018). The satellite products were used to fill the temporal and spatial gaps in the data of NMA and to get better continuous data of better quality. This combined dataset has better data quality in Ethiopia's National observation Esayas et al. (2018) with no missing data. The combined data were used for the historical drought analysis.

For the future drought characterization, Statistical Downscaling Model (SDSM) was used for the future simulation of temperature and rainfall using two scenarios, namely Representative Concentration Pathways (RCPs) 4.5 and 8.5. SDSM is a decision support tool that facilitates the assessment of regional impacts of global warning by allowing spatial-scale reduction of data provided by the large-scale Global Climate Model (GCM) (Wilby et al., 2002). The software of SDSM is accessed from the website.[1]

SDSM is categorized as a hybrid model and used to downscale the output from a GCM by emerging a statistical relationship among the local (predictands) and large-scale climate variables (predictors) by applying a multi-linear regressions model and stochastic bias correction techniques (Wilby & Dawson, 2007, 2015). The GCM's outputs (named as predictors) are used for a single station's linear condition and non-condition the local-scale weather generator parameters. Rainfall is a conditional process modeled using a stochastic weather generator conditioned on the predictor variables. The maximum and minimum temperature is a non-conditional process. It is modeled using a stochastic weather generator non-conditioned on the predictor variables. The projection from the second-generation Canadian Earth System Model (CanESM2), which is the fourth-generation coupled global climate model developed by the Canadian Centre for Climate Modeling and Analysis (CCCma) of Environment and Climate Change Canada, was used in this study.[2] The predictors derived starting CanESM2 and the NCEP reanalysis data were exported into the SDSM directory for model calibration, validation, and projection according to the method given by Kalnay et al. (1996). Time series monthly IOD, SOI, and ENSO (NINO3.4) data (1983–2016) were obtained from the National Oceanic and Atmospheric Administration (NOAA) satellite mission website.[3]

2.3 Data analysis

2.3.1 Calculating drought indices (SPI and SPEI)

In this study, the Standard Precipitation Index (SPI) and the Standard Precipitation and Evaporation Index (SPEI) of ten climate stations for 4- and 12-month timescales were

---

[1] https://sdsm.org.uk/software.html

[2] https://climate-scenarios.canada.ca/?page=pred-canesm2

[3] https://psl.noaa.gov/gcos_wgsp/Timeseries/

computed using the "SPEI package" program written freely available in R-software. The computations were done for the historical (1983–2016) and future (2020–2100) following the methods of (Vicente-Serrano et al., 2012) and (Beguería et al., 2014). ArcGIS 10.5 was used for the spatial analysis.

Due to the complexity of drought and its wide impacts, adequate characterization of drought conditions generally requires the integration of different drought-related variables or indices (Hao & Singh, 2015). SPI was developed by (Mckee et al., 1993). It has advantages such as its sole dependence on precipitation data alone, its ability to evaluate drought on multiple time scales, and its appropriateness for comparing drought conditions between different periods (Tsakiris & Vangelis, 2005). Based on Mckee et al. (1993), the gamma function is defined based on probability density function as:

$$g(x) = \frac{1}{\beta^{\alpha}\Gamma(\alpha)}X^{\alpha-1}e^{-X/\beta}, \ \text{ for } X > 0 \tag{1}$$

where $\beta > 0$, is a scale parameter; $\alpha > 0$, is a shape parameter; $X > 0$, is the precipitation amount; and the gamma function is defined as $\Gamma(\alpha) = \int_{0}^{\infty} y^{\alpha-1}e^{-y}dy$

The commutative probability of precipitation is calculated as:

$$G(x) = \int_{0}^{x} g(x)dx = \frac{1}{\hat{\beta}^{\hat{\alpha}}\Gamma(\hat{\alpha})}\int_{0}^{x} X^{\hat{\alpha}-1}e^{-X/\hat{\beta}}dx \tag{2}$$

As the gamma function is undefined for $x = 0$, the commutative probability becomes:

$$H(x) = q + (1 - q)G(x)$$

where q is the probability of zero precipitation given by $q = m/n$, m is the number of zeros in precipitation, and n is the number of precipitation observations in the time series.

The commutative probability, $H(x)$, which is commutative probability is transformed to the standard normal random variable Z with mean of zero and variance of one, which is the value of the SPI. Therefore the SPI is computed by:

$$SPI = z = -\left(t - \frac{2.515517 + 0.8022853t + 0.010328t^2}{1 + 1.432788t + 0.189269t^2 + 0.001308t^3}\right) \tag{3}$$

where $t = \sqrt{\ln\left(\frac{1}{[H(x)]^2}\right)}$ for $0 < H(x) \le 0.5$

$$SPI = z = +\left(t - \frac{2.515517 + 0.8022853t + 0.010328t^2}{1 + 1.432788t + 0.189269t^2 + 0.001308t^3}\right) \tag{4}$$

where $t = \sqrt{\ln\left(\frac{1}{[1-H(x)]^2}\right)}$ for $0.5 < H(x) \le 1.0$

Unlike SPI, SPEI is based on precipitation and potential evapotranspiration (PET), which describes the degree of deviation between dry and wet conditions by standardizing the difference between PET and precipitation. In this study, the PET was used based on the Hargreaves method since some of the stations did not have complete data to satisfy the FAO recommended Penmann–Montieth method (Allen et al., 1998; Hargreaves et al., 2003). The Hargreaves technique needs only precipitation, maximum and

minimum temperatures, latitude, and extraterrestrial radiation (R_a) (Hargreaves et al., 2003). The Hargraves method was used to estimate the PET as follows.

$$\text{PET}_{\text{HG}} = 0.0023 \times \left(T_{\text{mean}} + 17.8\right) \times \left(\sqrt{T_{\text{max}} - T_{\text{min}}}\right) \times R_a \tag{5}$$

PET_{HG} is potential evapotranspiration (mm/day) evaluated using of Hargreaves method, R_a is the extraterrestrial radiation (mm/day) obtained theoretically as a function of latitude, T_{eman} is the average temperature (°C), and T_{max} and T_{min} are the maximum and minimum temperatures (°C), respectively. After PET was calculated, the difference between precipitation and PET (D_i) was estimated.

$$D_i = P_i - PET_i \tag{6}$$

D_i is climatic water balance (CWB) in a given period (mm), PET_i is the monthly potential evapotranspiration (mm), and P_i is the monthly precipitation in a given period (mm). The accumulated difference between PET and P in different time scales can be evaluated as

$$D_n^k == \sum_{i-0}^{k-1} \left(P_{n-i} - PET_{n-i}\right) \tag{7}$$

where n is the number of calculations and k is a different time scale. According to Vicente-Serrano et al. (2010), the log-logistic distribution functions give better results than other distributions for estimating SPEI series in standardized D with a standard deviation of one and mean of zero. The equation is given as:

$$f(x) = \frac{\beta}{\alpha}\left(\frac{x - \gamma}{\alpha}\right)^{\beta-1}\left[1 + \frac{x - \gamma}{\alpha}\right]^{-2} \tag{8}$$

The parameters β, α, and γ are shape, scale, and location parameters, respectively, for D values in the range ($\gamma < D < \infty$). Thus, the probability distribution function can be stated as

$$F(x) = \frac{\beta}{\alpha}\left[1 - \frac{\alpha}{x - \gamma}\right]^{-1} \tag{9}$$

The SPEI can easily be found as the standardized $F(x)$ with an estimation of

$$SPEI = W_i - \frac{2.515517 + 0.8022853W_i + 0.010328W_i^2}{1 - 1.432788W_i + 0.189269W_i^2 + 0.001308W_i^3} \tag{10}$$

The equation works regardless of whether p is greater than 0.5 or less or equal to 0.5. The equation is given as:

$$W_i = \begin{cases} \sqrt{-2\ln(p)} & \text{for } p \leq 0.5 \\ \sqrt{-2\ln(1-p)} & \text{for } p > 0.5 \end{cases} \tag{11}$$

where W_i is a probability weighted moment.

2.3.2 Determinations of drought characteristics

The frequency, duration, magnitude/severity, and intensity were calculated for all the climate stations based on Polong et al. (2019) and Zambreski et al. (2016).

The frequency of occurrence (F_s) is defined as

$$F_s = \frac{n_s}{N_s} \times 100\% \tag{12}$$

In the equation, n_s is the number of drought events (for SPI and SPEI < -1.0), N_s is the total number of months for the study period, and s specifies a climate station.

Magnitude is the index value's cumulative sum (Mg) based on the duration extent.

$$M_g = \sum_{i=1}^{N} I_i \tag{13}$$

The equation N represents the duration, and I_i represents either SPI or SPEI.

Intensity Events with a shorter duration and higher severities will have large intensities.

$$I = \frac{M_g}{\text{Duration}} \tag{14}$$

The M_g represent magnitude.

2.3.3 Mean seasonal drought trend

Since the SPI and SPEI have a serial correlation consequence, so may not be a straight use of the Mann–Kendall (MK) test. So, when data are not random and influenced by auto-correlation, Modified Mann–Kendall tests are used in trend detection. Hamed and Rao (1998) have proposed a variance correction approach to address the issue of serial correlation in trend analysis. Parametric trend testing requires that data be independent and routinely distributed, while nonparametric trend testing requires that the data be independent only (Hamed & Rao, 1998). The nonparametric trend is widely used in many subjects and is useful for detecting significant trends. The nonparametric approaches were used, namely the Modified Mann–Kendall test for serially correlated data using the Hamed and Rao (1998) variance correction approach. This method is particularly useful in studying trends. On completion of the trend, the process was carried out by the package "modified" in RStudio, which is used to perform the nonparametric Mann–Kendall test, Spearman′s rank correlation coefficient test, and all modified versions of the Mann–Kendall test (Pataka-muri, 2021; Patakamuri et al., 2020).

2.4 Model performance

The model performance indicators were calculated using Goodness-of-Fit Functions (GOF) (Zambrano-Bigiarini, 2020). During the calibration and validation of the SDSM, the performance of the time series was tested by using coefficient of determination (R^2), Pearson's correlation coefficient (r), Nash–Sutcliffe Efficiency (NSE), and percentage bias (PBIAS) which are defined by Zehtabian et al. (2016) for R^2, Gupta et al. (2009); Moriasi et al. (1983); Nash and SutCLIFFF (1970) for NSE, and Gupta et al. (2009) for PBIAS. The formula of R^2, NSE, and PBIAS one by one is as follows.

R^2 is expressed as by Zehtabian et al. (2016)

Table 2 Statistical performance values obtained during calibration and validation of rainfall and maximum and minimum temperatures of the upper Awash Basin

Parameter	The test is done for	Model performance test parameters			
		r	R^2	NSE	PBIAS
Rainfall	Calibration	0.72	0.51	− 0.67	− 16.4
	Validation	0.65	0.42	− 0.34	11.9
T_{max}	Calibration	0.95	0.91	0.66	− 0.1
	Validation	0.96	0.92	0.51	− 2.2
T_{min}	Calibration	0.96	0.92	0.87	− 0.1
	Validation	0.97	0.95	0.79	− 3.4

T_{max} = maximum temperature and T_{min} = minimum temperature

$$R^2 = \left[\frac{\left[\sum_{i=1}^{n} \left(x_i^{sim} - \bar{x}_{sim} \right) * \left(x_i^{obs} - \bar{x}_{obs} \right) \right]^2}{\sum_{i=1}^{n} \left(x_i^{sim} - \bar{x}_{sim} \right)^2 \sum_{i=1}^{n} \left(x_i^{obs} - \bar{x}_{obs} \right)^2} \right]; \ 0 \leq R^2 \leq 1 \tag{15}$$

In the equation, n is the number of observations in the period under consideration, x_i^{obs} is the ith observation of the constituent being evaluated, x_i^{sim} is the ith simulated value for the constituent being evaluated, and $\bar{x}_{sim}$ and $\bar{x}_{obs}$ are the mean of simulated and observed data, respectively.

The equation for NSE is given (Gupta et al., 2009; Moriasi et al., 1983; and Nash & SutCLIFFFF, 1970):

$$NSE = 1 - \left| \frac{\sum_{i=1}^{n} \left(x_i^{obs} - x_i^{sim} \right)^2}{\sum_{i=1}^{n} \left(x_i^{obs} - x^{mean} \right)^2} \right| \tag{16}$$

The x^{mean} is the mean of observed data for the constituent being evaluated, and the others are as defined in Eq. (15).

PBIAS is calculated by Gupta et al. (2009) as:

$$PBIAS = \left| \frac{\sum_{i=1}^{n} \left(x_i^{obs} - x_i^{sim} \right) \times 100}{\sum_{i=1}^{n} x_i^{obs}} \right| \tag{17}$$

Again the variables are as defined in Eq. (15).

3 Results

3.1 Downscaled climate data under RCP 4.5 and RCP8.5 Scenarios

The downscaling of the GCMs was performed using Statistical Downscaling Model (SDSM), with all the models indicating a higher accuracy at daily and monthly scales when evaluated using statistical indicators. We start this section by presenting the predictor suites generated for SDSM at each station for calibration using the data of 1983–2000. Next, we validated using the data from 2001 to 2016. The model's performance during calibration and validation is presented in Table 2. The RCPs consists of four independent

Table 3 Climatic Moisture categories based on SPI and SPEI values (Shekhar & Shapiro, 2019)

Categories	SPI and SPEI values
Extreme Drought	≤ -2.00
Severe Drought	-1.50 to -1.99
Moderate Drought	-1.00 to -1.49
Normal	0.99 to -0.99
Moderate Wet	1.00 to 1.49
Severe Wet	1.50 to 1.99
Extreme Wet	≥ 2.00

pathways: RCP 8.5 (high emissions), RCP 6.0 (intermediate emissions), RCP 4.5 (intermediate emissions), and RCP 2.6 (low emissions) (Ho et al., 2012). This study used RCP 4.5 and RCP 8.5 for future prediction. The results of RCP 8.5 and PCP4.5 from 2020 to 2100 were simulated using SDSM and used in this study. Based on data available in the study area, the observed data from 1983 to 2016 of the ten stations were used. The statistical performance of calibration results for the UAB between the observed rainfall, T_{max}, and T_{min} and those counterparts from the downscaling model is presented in Table 2.

It can be detected from Table 2 that the r, R^2, NSE, and PBAIS for rainfall obtained during calibration were 0.72, 0.51, -0.67, and -16.40, respectively. Corresponding values for T_{max} were, 0.95, 0.91, 0.66, and -0.1, respectively. Finally, the statistical performance of T_{min} for calibration showed 0.96, 0.92, 0.87, and -0.1 for r, R^2, NSE, and PBAIS, respectively. Thus, those results found from calibration can be used for the validation phase. The results of the validation for the statistical test parameters of r, R^2, NSE, and PBAIS showed 0.65, 0.42, -0.34, and 11.9 for rainfall, 0.96, 0.92, 0.51, and -2.2 for T_{max}, and 0.97, 0.95, 0.79, and -3.4 for T_{min}, respectively. In general, the results showed a good performance of SDSM in modeling rainfall during the calibration and satisfactory during validation, with excellent results for maximum and minimum temperatures during both the calibration and the validation phases. Positive correlations were obtained between observed and simulated for all three parameters. The maximum negative PBAIS of -16.4 obtained during rainfall calibration indicates an overestimation of the simulated rainfall. However, it is very small and does not affect the future prediction of the rainfall. The statistical performance results of the validation period are almost similar to those of the calibration period. Therefore it can be concluded that the performance of the calibrated model is representative and can be used in the future projection of RCP8.5 and RCP4 for the years 2020–2100 using SDSM for rainfall, the maximum and the minimum temperatures.

3.2 Spatial and temporal drought pattern and characteristics in the basin from 1983 to 2016

The time series of the SPI and SPEI at 4- and 12-month timescales were calculated using observed climate data from 1983 to 2016. The dryness categories used in the results are based on Table 3.

From the analysis of both indices, for the mean of UAB, the peak value of magnitude and intensity are presented for SPI12 and SPI4 of -89.125 and -3.02, respectively (Table 4).

Table 4 Duration, severity, and intensity occurrence of the major dry (SPEI ≤ − 1) events over the basin during 1983–2016

Drought Index	Duration	Severity/Magnitude	Intensity	Highest Value	Drought Index	Duration	Severity/Magnitude	Intensity	Highest value
SPI4	36	− 61.245	− 1.701	− 3.02	SPI12	57	− 89.125	− 1.564	− 3.67
SPEI4	55	− 78.501	− 1.427	− 2.08	SPEI12	47	− 73.372	− 1.561	− 2.3

Table 5 The duration, severity, and intensity of occurrence of some of the major dry events (SPI and SPEI ≤ -1)

Station	Drought index	Period of dry occurrence	Duration	Severity	Intensity	Highestvalue	Drought Index	Period of dry occurrence	Duration	Severity	Intensity	Highest value
Addis Ababa Bole	SPI4	Aug 1995-Dec 1995	5	−7.98	−1.60	−3.03	SPI12	Jun 2014-May 2015	12	−20.67	−1.72	−2.77
	SPEI4	Feb 2015-Jul 2015	6	−8.55	−1.43	−2.65	SPEI12	Jun 2014-Dec 2016	31	−49.37	−1.59	−2.23
Addis Alem	SPI4	Feb 1984-Nov 1984	10	−14.64	−1.46	−2.54	SPI12	Apr 2015-Apr 2016	13	−19.14	−1.47	−2.58
	SPEI4	Feb 2015-Apr 2016	15	−26.59	−1.77	−2.53	SPEI12	Apr1984-Feb 1986	23	−34.58	−1.50	−2.28
Asgori	SPI4	Aug 1983-Jan 1984	6	−7.78	−1.30	−2.79	SPI12	Aug 2012-Aug 2013	13	−18.36	−1.41	−2.49
	SPEI4	Mar 2015-Mar 2016	13	−21.05	−1.62	−3.21	SPEI12	Jul 2015-Dec 2016	18	−30.78	−1.71	−2.34
Koka Dam	SPI4	May 1991-Sep 1991	5	−8.14	−1.63	−2.77	SPI12	Dec 1983-May 1986	30	−42.06	−1.40	−1.81
	SPEI4	Sep 2005-Feb 2006	6	−8.71	−1.45	−2.74	SPEI12	Mar 1984-May 1986	27	−35.47	−1.31	−1.99
Ginchi	SPI4	Jul 1984-Jan 1985	7	−11.50	−1.64	−2.51	SPI12	Sep 2011-Apr 2013	20	−28.71	−1.44	−2.29
	SPEI4	Feb 2015-Jan 2016	12	−17.90	−1.49	−2.08	SPEI12	Oct 2014-Jul 2016	22	−34.55	−1.57	−2.18
Hombole	SPI4	Jul 1987-Dec 1987	6	−11.38	−1.90	−3.13	SPI12	Jun 2002-May 2003	12	−21.92	−1.83	−3.50
	SPEI4	Jun 2002-Dec 2002	7	−11.62	−1.66	−2.21	SPEI12	Jun 2002-Jun 2003	13	−28.89	−2.22	−3.22
Kimoye	SPI4	Apr 1999-Sep 1999	6	−9.11	−1.52	−2.96	SPI12	Aug 1984-Jul 1985	12	−18.68	−1.56	−3.05
	SPEI4	Feb 2015-Apr 2016	15	−26.42	−1.76	−2.36	SPEI12	Apr 2015-Dec 2016	21	−35.26	−1.68	−2.22

Table 5 (continued)

| Station	Drought index	Period of dry occurrence	Duration	Severity	Intensity	Highestvalue	Drought Index	Period of dry occurrence	Duration	Severity	Intensity	Highest value
Mojo	SPI4	Mar 2002-Sep 2002	7	−11.93	−1.70	−3.15	SPI12	Mar 2002-Feb 2003	12	−22.33	−1.86	−2.47
	SPEI4	Jan 2011-Aug 2011	8	−12.81	−1.60	−2.32	SPEI12	Apr 2002-Mar 2003	12	−21.21	−1.77	−2.27
Sendafa	SPI4	Apr 2009-Nov 2009	8	−13.10	−1.64	−4.16	SPI12	Aug 1991-Jul 1992	12	−20.20	−1.68	−2.62
	SPEI4	Jun 2015-Feb 2016	8	−11.63	−1.45	−2.42	SPEI12	Aug 2015-Jul 2016	12	−22.33	−1.86	−2.16
Tulu Bolo	SPI4	Jul 1987-Dec 1987	6	−7.84	−1.31	−2.25	SPI12	Jul 1991-Mar 1992	9	−11.08	−1.23	−2.09
	SPEI4	Feb 2015-Oct 2015	9	−12.79	−1.42	−2.29	SPEI12	Aug 2015-Apr 2016	9	−17.88	−1.99	−2.36

In Table 4, the drought intensity is severe (− 1.5 to 1.9) for three indices (SPI4, SPI12, and SPEI12) and moderate for SPEI4. Table 5 highlights the evolution of dry events for some significant cases over UAB in the past 34 years with an analysis of SPI and SPEI for 4 and 12 months. The table displays the drought characteristics observed in UAB.

From Table 5, one can also see the same result of moderate to severe droughts as observed in Table 4, except in one case (Hombole) in which extreme drought intensity of − 2.22 was observed between June 2002 and June 2003. The extended consecutive dry events for SPI-4 occurred in Addis Alem (10 months) from February to November 1984. The dry event's most prolonged continuous drought duration of 37 series months of drought duration was observed at Koka Dam station for SPI-12. For the SPEI-4 drought index, the maximum consecutive dry event was observed in Addis Alem and Kimoye for 15 months. For SPEI-12, the long duration of the dry event was detected in Addis Ababa Bole, lasting for 27 months. Moreover, the highest intensity of SPI for 4 and 12 months was observed at Hombole (− 1.896) and Mojo (− 1.861), respectively. For the case of SPEI 4- and 12-month timescales, the maximum intensity was observed in Addis Alem (− 1.773) and Tulu Bolo (− 1.987), respectively. Generally, in the basin, the maximum severity and intensity of − 49.37 and − 2.22 occurred from 1983 to 2016 at Addis Ababa Bole and Hombole climate stations, respectively.

The threshold value used in this study to estimate the temporal and spatial variation of drought events in the basin is consecutively less than a threshold value (SPI ≤ − 1 and SPIE ≤ − 1). The spatial patterns of the frequency of dry cases of the SPI and SPEI for 4 and 12 months are presented in Fig. 2.

From the spatial analysis of Fig. 2, the highest drought frequency was observed for SPEI4 (Fig. 2c) in the northwest and decreased in the eastern and southeast parts. The results of Fig. 2a indicate that the highest frequency of dry events for SPI-4 was observed over the past 34 years in the central northwest part of the basin (around Addis Alem, Kimoye, and Asgori), whereas the southwestern part (Hombole and Tulu Bolo) exhibited rare drought events. The remaining parts of the basin also observed a low frequency of dry events for SPI-4. For the long-term (SPI-12 shown in Fig. 2b), the study area experienced moderate drought frequencies in the western and southern parts and low frequency in the northeastern part. Figure 2d (SPEI-12) drought frequency was exhibited at the southeastern tip of the basin. Except for the northeast and southwest, which experienced moderate drought frequencies, the rest of the basin had low drought frequencies of SPEI-12. From 1983 to 2016, the basin experienced 12% to 19.8% moderate and above moderate drought frequencies in both SPI and SPEI for all the timescales. Overall, from Fig. 2a higher frequency of drought events was observed for SPI4 and the SPEI4 almost in all parts of the basin.

As far as SPI4 is concerned (Fig. 2e), extreme droughts occurred 6 times from 1983 to 2016 during 1984, 1987, 2001, 2008, 2009 and 2015. The time gap between consecutive drought years ranges from one to 6 years. The severe droughts for the same index occurred 8 times (1986, 1991, 1994, 1995, 1999, 2000, 2013, and 2014). The severe drought had time gaps ranging from 1 to 12 years. Drought occurrence for years in a row tends to increase the time gap. For instance, after the severe drought years of 1994/1995, the next drought occurred 3 years later (in 1999). Similarly, after the drought years of 1999/2000, the next drought occurred after 12 years (in 2013). As far as this drought index is concerned, the decade 2000–2009 had benign years compared to the 1990–1999 decade. SPI 12 showed only 3 extreme cases (1988, 2015, and 2016) from 1983 to 2016 and 6 severe cases in 1984, 1985, 1995–1997, and 2002. The comparison of SPI4 with SPI12 indicates
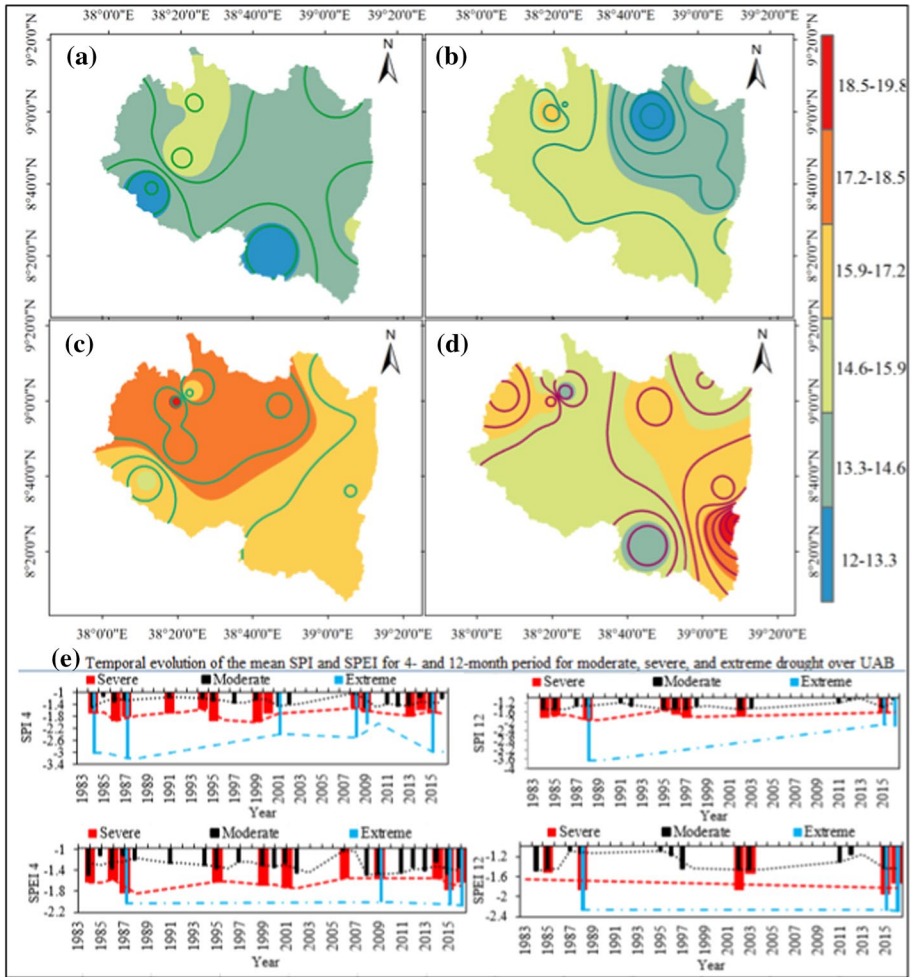
Fig. 2 The spatial variability in drought frequency (%) in **a** SPI-4, **b** SPI-12, **c** SPEI-4, and **d** SPEI-12 of the ten stations of UAB (1983–2016)

that SPI12 occurred in about half of SPI4 in extreme and 75% in severe droughts. The two coincided with extreme drought in 2015 and severe drought in 1995.

SPEI4 analysis showed 4 years of extreme drought events (1987, 2009, 2015 and 2016) and 7 years of severe drought events (1984, 1986, 1995, 1999, 2001, 2006 and 2014). The SPEI12, on the other hand, showed 3 years of extreme drought events (1988, 2015 and 2016) and three years of severe drought events (1985, 2002 and 2003). SPEI4 and SPEI12 coincided in extreme drought events during 2015 and 2016 and no coinciding years in severe drought events. SPI4 and SPEI4 in extreme drought events showed coincidence in 1987, 2009 and 2015. In the case of severe drought events, the two coincided for 4 years (1986, 1995, 1999 and 2014). Whenever such coincidences occur, it could be concluded that those years were drought years. The year 2001 was an extreme drought year in SPI4 but was downgraded as a severe drought year by SPEI4. Comparisons of SPI12 and SPEI 12 indicate complete agreement in the
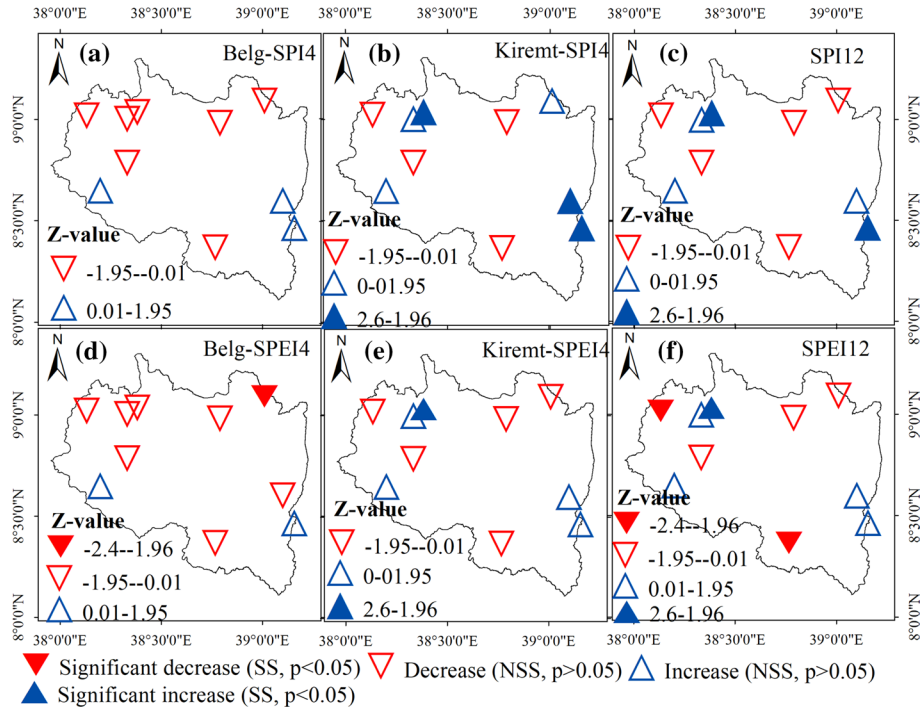
Fig. 3 Seasonal drought trend using SPI and SPEI from 1983 to 2016

extreme drought event years 1988, 2015 and 2016. Thus SPI and SPEI gave the same result, and the years were drought years. In the case of severe drought, agreements were observed in 1985 and 2002. Moreover, 1984 and 1995–1997 had severe droughts according to SPI12 and only 2003 as far as SPEI12 is concerned.

3.3 Seasonal drought trend of the basin during 1983–2016

Figure 3 shows the historical seasonal trend of drought indices using Z-values and Sen's slope estimators in the UAB. Note that in the analysis of the drought trend, the negative values of Z characterize drying tendency, whereas the positive indicates a wetting trend. Even though there are drying trends in almost all stations, SPI4 and SPEI4 do not show any significant increasing or decreasing drought trends in Belg (FMAM) season as indicated by Z-values except in Sendafa showed a significant increase in drought (SPEI4). Kiremt (JJAS) season SPI4 and SPEI4 drought trends show similarity in almost all stations, except in the eastern part of the basin, where the SPI4 fails to show a significant decrease in SPEI shows a significant decrease in drought. SPI12 and SPEI12 show similarities in the north, west, and central parts and slight differences in the southeast. Overall, along the diagonal from southeast to northwest, there seems to be a reduction in drought while it is almost uniform for the other parts.

Table 6 The duration, severity, and intensity occurrence of the major dry (SPEI ≤ − 1) events over the basin during 2020–2100

Drought Index	Duration (month)	Severity	Intensity	Highest value	Drought Index	Duration (month)	Severity	Intensity	Highest value
SPI4_RCP4.5	106	− 164.01	− 1.55	− 3.50	SPI12	162	− 257.89	− 1.59	− 3.06
SPEI4_RCP4.5	113	− 174.47	− 1.54	− 3.10	SPEI12	186	− 267.86	− 1.44	− 2.37
SPI4_RCP8.5	133	− 183.40	− 1.38	− 2.88	SPI12	135	− 178.53	− 1.32	− 2.09
SPEI4_RCP8.5	134	− 197.63	− 1.48	− 2,99	SPEI12	153	− 208.00	− 1.36	− 2.18

3.4 Future patterns of drought using SPI and SPEI and scenarios

The duration, severity, and intensity occurrence of the major dry (SPEI ≤ -1) events over the basin during 2020–2100 are calculated and given in Table 6.

With scenario RCP4.5, the future trend shows a slight decrement in the intensity of drought in 5 out of the ten, intensity values are moderate, and even the ones categorized as severe are close to the moderate than extreme. Thus the overall trend shows more reduction in drought intensity than in the present or the past.

3.5 Future temporal patterns of drought using SPI and SPEI and RCP4.5 scenario

Table 7 highlights the evolution of dry events for some notable cases over UAB to analyze SPI and SPEI for 4- and 12-month of the RCP4.5 scenario from 2020-to 2100.

As shown in the table, prolonged duration of the dry event for SPI-4 that lasted 17 months was observed in Ginchi. From the analysis of drought, the driest event for SPI-12 was experienced from April 2021-June 2025 in Addis Alem, with the duration of occurrence persisting for 51 months for both SPEI 4- and 12-month timescale. The highest magnitude and intensity of SPI and SEI for 4- and 12-month were also noted in Addis Alem and Koka dam stations at -83.50 and -2.37, respectively. Based on this scenario, the overall intensity of drought will increase severely and some extreme. SPI4 predicts extreme drought in four of the ten stations. SPEI4, on the other hand, predicts only in one of the ten stations. As far as SPI12 is concerned, only one of the ten stations will experience extreme drought, but none, according to the SPEI12. The result of SPEI is more optimistic in both cases.

3.6 Future temporal patterns of drought using SPI and SPEI and RCP8.5 scenario

The evolutions of dry events for some notable cases of SPI and SPEI for 4 and 12 months for the RCP8.5 scenario were analyzed over UAB (Table 8). The extended duration of the dry event for SPI-4 RCP8.5 will be detected at Tulu Bolo climate station at 29 months and for SPI-12 RCP8.5 in Koka Dam station (37 months). From the analysis of drought, the driest event for SPEI for 4- and 12-month timescales, the highest duration of dry events will be observed in Tulu Bolo (25 months) and Ginchi and Tulu Bolo (36 months), respectively. Regarding the highest intensity of dry events for the highest scenario in the future, SPI-4 and SPI-12 will be detected in Addis Ababa Bole (-2.348) and Humble (-1.777) stations, respectively. Mojo (-2.106) and Sendafa and Hombole will observe -1.91 for SPEI-4 and SPEI-12 months. In the basin, the highest magnitude and intensity of -46.13 and -2.35 will be observed at Tulu Bolo and Addis Ababa Bole stations, respectively, for the 4-month timescales.

According to SPI4 extreme drought, events will be observed in this scenario at four out of the ten stations. Prediction by SPEI4 indicates only one station (Mojo). Of the severe drought events predicted by the two, five are by SPI4 and seven by SPEI4. Most of the extreme dry events predicted by SPI4 are reduced to severe by SPEI4 prediction. None of the SPI12 and SPEI12 predicted extreme dry occurrence for all the ten stations. Severe drought occurrence will be observed in four out of the ten stations based on SPI12 and in five of the ten stations based on SPEI12. The two predict severe dryness in three stations

Table 7 The duration, severity, and intensity of some of the major dry events (SPI and SPEI ≤ − 1) of the ten stations for the RCP4.5 scenario during 2020–2100

Station	Drought Index	Period of dry occurrence	Duration	Severity	Intensity	Highest value	Drought Index	Period of dry occurrence	Duration	Severity	Intensity	Highest value
Addis Ababa Bole	SPI4	Apr 2029-Dec 2029	9	− 17.99	− 2.00	− 2.56	SPI12	May 2024-Mar 2026	23	− 35.53	− 1.55	− 2.78
	SPEI4	Apr 2021-Jan 2022	10	− 16.77	− 1.68	− 2.64	SPEI12	Apr 2024-Mar 2026	24	− 35.35	− 1.47	− 2.35
Addis Alem	SPI4	Mar 2029-Feb 2030	12	− 25.19	− 2.10	− 4.27	SPI12	Apr 2021-Jun 2025	51	− 83.50	− 1.64	− 3.04
	SPEI4	Mar 2029-Mar 2030	51	− 23.03	− 1.77	− 2.72	SPEI12	Apr 2021-Jun 2025	51	− 78.01	− 1.53	− 2.26
Asgori	SPI4	Feb 2029-Oct 2029	9	− 16.84	− 1.87	− 2.84	SPI12	Feb 2028-Mar 2030	26	− 40.23	− 1.55	− 2.35
	SPEI4	Mar 2050-Feb 2051	12	− 17.45	− 1.46	− 2.93	SPEI12	Mar 2024-Apr 2026	24	− 44.58	− 1.71	− 2.14
Koka Dam	SPI4	Sep 2034-Nov 2035	15	− 21.31	− 1.33	− 3.43	SPI12	Sep 2023-Mar 2026	31	− 47.64	− 1.54	− 3.51
	SPEI4	Feb 2029-Dec 2029	11	− 26.03	− 2.37	− 2.48	SPEI12	Apr 2029-Oct 2031	31	− 54.87	− 1.77	− 2.38
Ginchi	SPI4	Sep 2020-Jan 2022	17	− 28.24	− 1.66	− 3.31	SPI12	Dec 2020-Aug 2022	21	− 42.44	− 2.02	− 3.45
	SPEI4	Jan 2021-Feb 2022	14	− 23.59	− 1.69	− 2.76	SPEI12	Jul 2052-May 2054	23	− 30.77	− 1.34	− 2.37
Hombole	SPI4	Mar 2029-Feb 2030	12	− 25.05	− 2.09	− 5.06	SPI12	Feb 2021-Dec 2023	35	− 57.74	− 1.65	− 2.64
	SPEI4	Apr 2029-Feb 2030	11	− 18.38	− 1.67	− 2.69	SPEI12	Jul 2081-Jul 2082	13	− 23.75	− 1.83	− 2.52
Kimoye	SPI4	Jan 2021-Jan 2022	13	− 21.65	− 1.67	− 3.51	SPI12	May 2024-Mar 2026	23	− 37.26	− 1.62	− 3.20
	SPEI4	Jan 2021-Jan 2022	13	− 21.88	− 1.68	− 4.29	SPEI12	Apr 2024-Mar 2026	24	− 35.34	− 1.47	− 2.79

Table 7 (continued)

Station	Drought Index	Period of dry occurrence	Duration	Severity	Intensity	Highest value	Drought Index	Period of dry occurrence	Duration	Severity	Intensity	Highest value
Mojo	SPI4	Apr 2029-Jan 2030	10	− 18.06	− 1.81	− 2.96	SPI12	Oct 2034-Sep 2036	24	− 41.17	− 1.58	− 2.65
	SPEI4	Apr 2029-Jan 2030	10	− 17.05	− 1.71	− 2.86	SPEI12	Oct 2034-Sep 2036	24	− 34.60	− 1.44	− 2.29
Sendafa	SPI4	Mar 2029-Feb 2030	12	− 24.03	− 2.00	− 4.46	SPI12	Oct 2034-Aug 2036	23	− 35.27	− 1.53	− 2.69
	SPEI4	Mar 2029-Feb 2030	12	− 20.80	− 1.73	− 2.60	SPEI12	Jan 2071-Jun2072	18	− 26.31	− 1.46	− 2.18
Tulu Bolo	SPI4	Jan 2024-Feb 2025	14	− 20.50	− 1.46	− 3.32	SPI12	Jun 2023-Mar 2026	34	− 56.78	− 1.67	− 2.64
	SPEI4	Feb 2029-Apr 2030	15	− 26.34	− 1.76	− 3.03	SPEI12	May 2023-Apr 2026	36	− 57.18	− 1.59	− 2.38

Table 8 The duration, severity, and intensity of occurrence of some of the major dry events (SPI and SPEI ≤ -1) of the ten stations for the RCP8.5 scenario during 2020–2100

Station	Drought Index	Period of dry occurrence	Duration	Severity	Intensity	Highest value	Drought Index	Period of dry occurrence	Duration	Severity	Intensity	Highest value
Addis Ababa Bole	SPI4	May 2031-Dec 2031	8	−18.79	−2.35	−3.38	SPI12	Jun 2058-Mar 2060	22	−25.93	−1.18	−2.62
	SPEI4	Mar 2021-Nov 2021	9	−13.81	−1.53	−3.65	SPEI12	Apr 2058-Mar 2060	24	−32.06	−1.34	−2.72
Addis Alem	SPI4	May 2031-Jan 2032	9	−20.66	−2.30	−3.38	SPI12	Apr 2021-Mar 2024	36	−51.35	−1.43	−2.81
	SPEI4	Mar 2021-Apr 2022	14	−23.73	−1.70	−3.13	SPEI12	May 2021-Dec 2023	32	−48.65	−1.52	−2.83
Asgori	SPI4	May 2026-Feb 2027	10	−17.68	−1.77	−2.39	SPI12	Apr 2021-Mar 2024	36	−50.16	−1.39	−2.02
	SPEI4	May 2026-Mar 2027	11	−19.30	−1.76	−2.30	SPEI12	Apr 2026-Dec 2027	21	−34.11	−1.62	−2.12
Koka Dam	SPI4	May 2034-Sep 2035	17	−24.68	−1.45	−2.63	SPI12	Mar 2021-Mar 2024	37	−49.56	−1.34	−1.92
	SPEI4	May 2034-Sep 2035	17	−24.88	−1.46	−2.65	SPEI12	Aug 2021-Mar 2024	32	−44.51	−1.39	−2.01
Ginchi	SPI4	Feb 2021-Jul 2022	18	−28.84	−1.60	−2.89	SPI12	Apr 2021-Mar 2024	36	−58.44	−1.62	−2.07
	SPEI4	Feb 2021-Jul 2022	18	−28.05	−1.56	−2.48	SPEI12	Apr 2021-Mar 2024	36	−56.46	−1.57	−2.32
Hombole	SPI4	May 2041-Feb 2042	10	−16.74	−1.67	−3.55	SPI12	May 2041-Mar 2042	11	−19.54	−1.78	−3.28
	SPEI4	Jan 2100-Aug 2100	8	−14.22	−1.78	−3.10	SPEI12	Sep 2067-Sep 2069	25	−47.74	−1.91	−2.44
Kimoye	SPI4	Mar 2021-Apr 2022	14	−21.46	−1.53	−3.25	SPI12	May 2021-Mar 2024	35	−50.43	−1.44	−2.61
	SPEI4	Apr 2021-Apr 2022	13	−20.75	−1.60	−2.74	SPEI12	May 2021-Mar 2024	35	−49.83	−1.42	−2.06

Table 8 (continued)

Station	Drought Index	Period of dry occurrence	Duration	Severity	Intensity	Highest value	Drought Index	Period of dry occurrence	Duration	Severity	Intensity	Highest value
Mojo	SPI4	May 2031-Nov 2031	7	−15.09	−2.16	−3.18	SPI12	Jun 2022-Mar 2024	22	−29.72	−1.35	−2.42
	SPEI4	May 2031-Dec 2031	8	−16.85	−2.11	−3.55	SPEI12	May 2059-Aug 2060	16	−22.27	−1.39	−2.55
Sendafa	SPI4	May 2031-Dec 2031	8	−16.46	−2.06	−3.06	SPI12	Feb 2031-May 2032	16	−27.89	−1.74	−2.39
	SPEI4	Mar 2021-Apr 2022	14	−18.24	−1.30	−3.24	SPEI12	Feb 2031-Jun 2032	17	−32.49	−1.91	−2.62
Tulu Bolo	SPI4	Jan 2021-May 2023	29	−46.13	−1.59	−2.83	SPI12	Apr 2021-Mar 2024	36	−54.89	−1.53	−2.56
	SPEI4	Feb 2028-Feb 2030	25	−41.63	−1.67	−2.29	SPEI12	Apr 2021-Mar 2024	36	−52.40	−1.46	−2.17
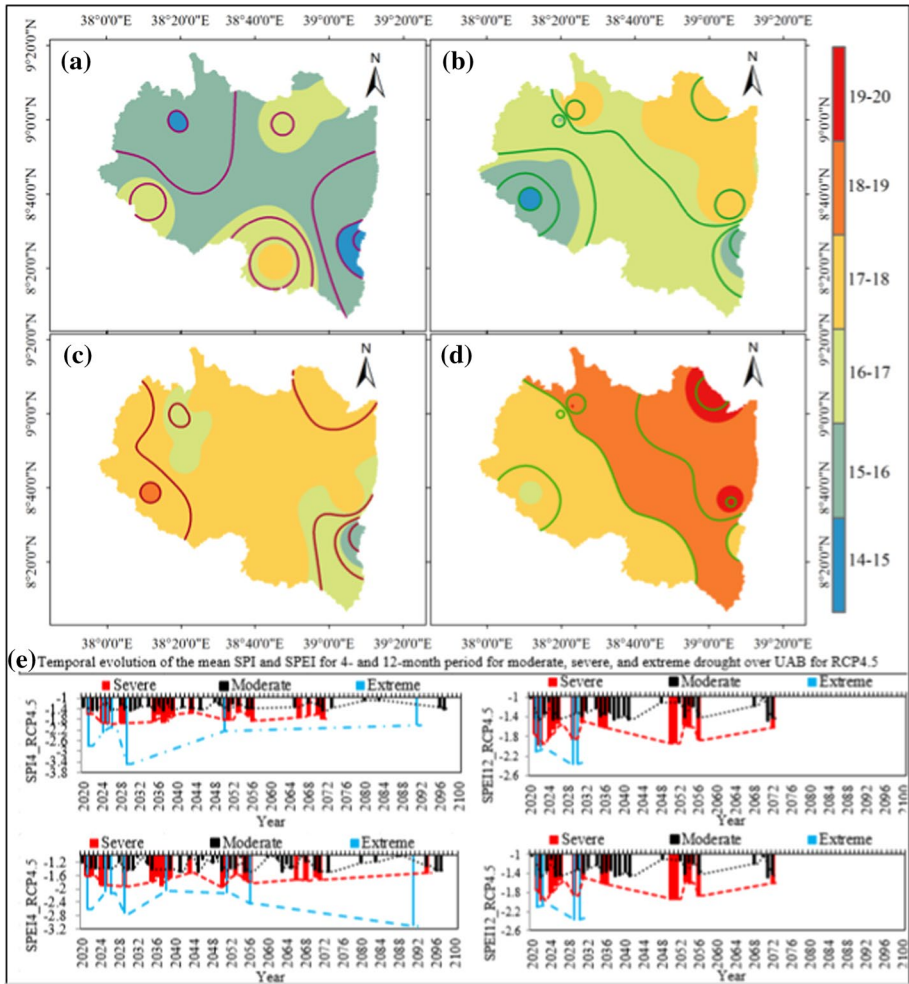
Fig. 4 The projected spatial changes in drought frequency (%) in **a** SPI4_RCP4.5, **b** SPI12-RCP4.5, **c** SPEI4-RCP4.5, and **d** SPEI12-RCP4.5 of the ten stations of upper Awash Basin from 2020 to 2100

(Ginchi, Hombole, and Sendafa). The absence of extreme drought and the reduction in severe drought (only moderate dryness at four stations) indicates more wetness, which is an optimistic scenario for the basin.

3.7 Future spatial (RCP4.5) and temporal patterns of drought using SPI and SPEI

The spatial pattern of the frequency of dry cases for the SPI and SPEI for 4- and 12-months periods are presented in Fig. 4 from a-d for RCP4.5 and Fig. 4e for both scenarios, respectively. In the case of SPI4_RCP 4.5 (Fig. 4a), drought frequency stayed low in the northwest, southeast, and central area and moderated in the northeast and southwest during the projection year. SPI12 for the same scenario (Fig. 4b) showed high frequency in the northeast, moderate frequency in the northwest, central, and southeast, and low in the west.

SPEI4_RCP4.5 (Fig. 4c) showed moderate drought in almost all stations, except for a few patches in southeast and northwest areas. On the other hand, SPEI12_RCP4.5 exhibited two distinct patterns: high frequency on the eastern side and moderate frequency on the western side with a clear northwest and southeast diagonal divide.

Comparing SPI4 with SPEI4 (Fig. 4a and c) and (Fig. 4b and d), one can see clear differences between the two in each case. The spatial prediction of SPI is more of mild/moderate drought, whereas that of SPEI is more severe. The temporal evolution of SPI4_RCP4.5 (Fig. 4e) shows six extreme drought events, out of which four will occur until 2030. The remaining two will occur with a time gap of about 40 years (one around 2050 and the other in 2092). Severe drought events will occur more frequently, but they also tend to have cyclic patterns. In the figure, the more frequent ones will occur in the 2030s, 2050s, and 2060s. This scenario does not indicate any severe drought after that. The prediction of SPEI4_RCP4.5 is almost identical to the SPI4_RCP4.5 with slight differences. SPEI4_RCP4.5, for instance, predicts two more extreme drought events (one in the 2030s and the other in the 2050s) that SPI4_RCP4.5 does not predict. SPEI12_RCP4.5 predicts no extreme drought event after 2030 even though severe drought continues to exist until 2072.

3.8 Future spatial (RCP8.5) and temporal patterns of drought using SPI and SPEI

Scenario RCP8.5 by SPI and SPEI is shown in Fig. 5a–d. The temporal evolution is given in Fig. 5e.

Scenario RCP8.5 by SPI4 (Fig. 5a) reveals a decline in drought frequency from west to east, with the least frequency in the northeast. SPEI4_RCP8.5 (Fig. 5c) also shows a decline from west to east, but the frequency of occurrence is not as slow as the one predicted by SPI4_RCP8.5. SPEI with the same scenario (Fig. 5b) shows a reduction from east and west to the center. SPEI12-RCP8.5 (Fig. 5d) shows high to very high drought frequency in the west, while it remains moderate for the rest of the watershed. A comparison of the two SPEI4 and SPEI12 shows that they both indicate similar trends, but the prediction of SPEI4 is more optimistic than that of SPEI12.

SPI4_RCP8.5 shows only two extreme droughts until the beginning of the 2030s and none after that. The severe drought stays until the mid-2040s and none after that. SPI12_RCP8.5 predicts a similar thing in extreme drought and ends the severe drought earlier (by the mid-2030s). SPEI4 and SPEI12 predict the end of extreme droughts in 2038 and 2032, respectively. For SPEI4, the severe drought lingers until the 2060s, whereas for SPEI12, it ends by the mid-2040s. Overall, the SPEIs predict worse conditions than the SPIs, even if they both predict a better future.

3.9 Future seasonal drought analysis (2020–2100) using RCP4.5 and RCP8.5 and linked with global climate indices

Analysis of drought on a seasonal basis is important to know the variability of the flow of the Awash River. Since the watershed includes areas with bimodal rainfall, the contribution of FMAM (Belg) rainfall could help sustain the river's flow during the dry season. Figure 6 shows the future trends in the two rainy seasons and annually.

As far as the future means drought trend for both SPI and SPEI for the RCP4.5 scenario, both SPI and SPEI predict similar things. For FMAM (Belg) season, there will not be any significant trend for most stations. SPI4 showed increasing trends, whereas SPEI showed
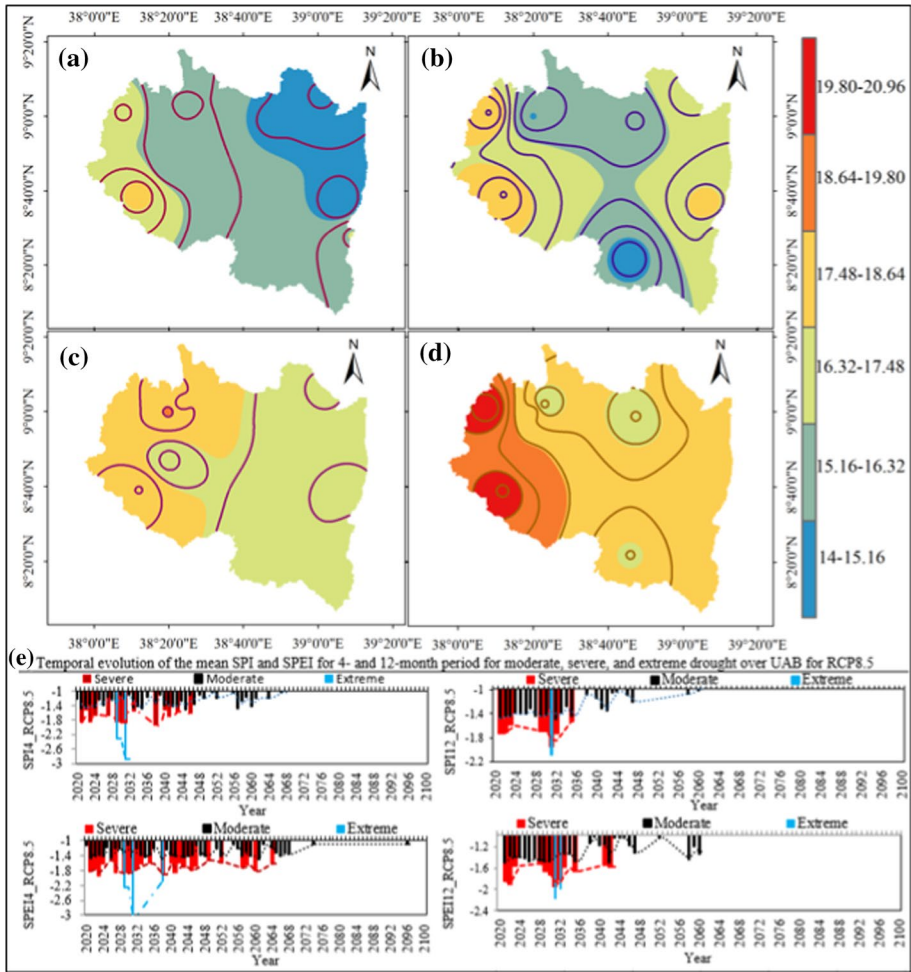
Fig. 5 The projected spatial changes in drought frequency (%) of **a** SPI4_RCP8.5, **b** SPI12-RCP8.5, **c** SPEI4-RCP8.5, and **d** SPEI12-RCP8.5 of the ten stations of upper Awash Basin from 2020 to 2100

only one with an increasing trend. Thus, there will not be a change in the future Belg season drought trend. The JJAS (Kiremt) season more or less dictates the annual trend since the two are showing similar trends of increasing Z-values for almost all of the stations in both SPI and SPEI. The differences between SPI4 and SPEI12 are in one station (Hombole), where there are increasing trends in Kiremt and annual SPI4 but none in SPI4 and SPEI12 (Fig. 6).

Figure 7 shows the future trends in the two rainy seasons and annually.

For the RCP 8.5 (highest emissions), it is apparent from Fig. 7 that except in one station (Hombole for SPEI), a significant wetting trend was revealed for Belg, Kiremt, and annual during 2020–2100. From both RCP4.5 and 8.5 trends, analysis for SPI/SPEI depicts the decreasing mean drought events and wetting will increase in the entire basin. Unlike what was observed in the RCP4.5 scenario, the RCP8.5 scenario showed an increasing trend for the Belg season. This result agrees with the analysis of the temporal
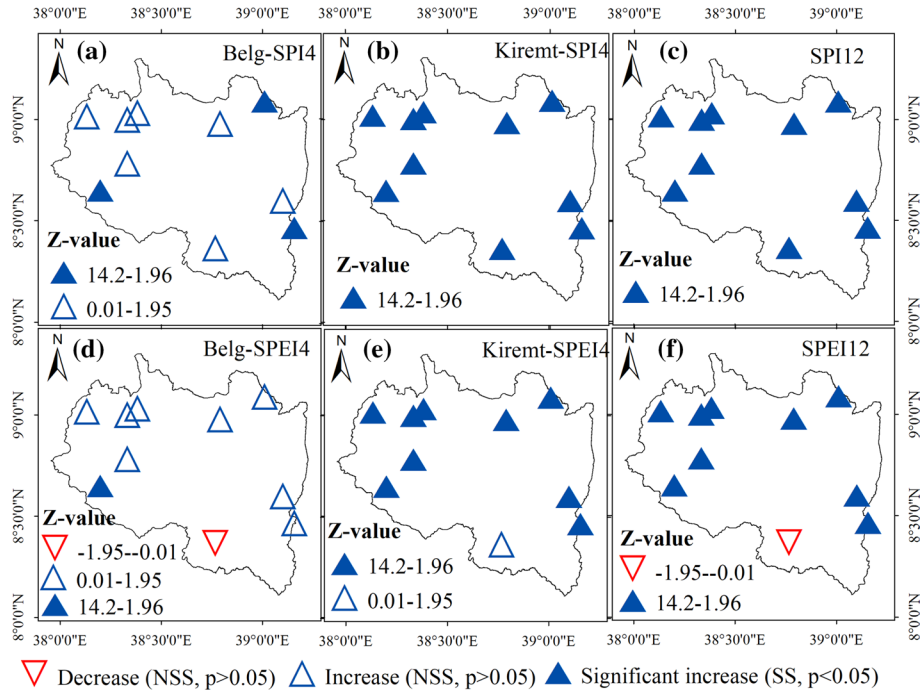
Fig. 6 Future seasonal drought trend of SPI and SPEI for RCP4.5 during 2020–2100

evolution of drought that showed drought events that show a decrease from 2060 to 2100, but shortly, the evolution indicates the tendency of drought will increase.

In this study, attempts were made to see the links between the two drought indices (SPI and SPEI) with the global climate indices (IOD, SOI, and ENSO). Figure 8 shows how the drought indices and the global climate indices are related to the basin as a whole. The correlation is based on Pearson's correlation coefficient (r).

Based on Fig. 8, the correlation between IOD and Belg season is positive. Similarly, there is a weak negative correlation with Kiremt season. Thus it can be concluded that the link between IOD and drought indices is weak for both seasons. The southern oscillation index is positively correlated with Kiremt SPI4 and SPEI4, but a negative correlation of lower magnitude with Belg season. ENSO (Nino3.4) seems to have a good positive correlation with Belg SPI4 and SPEI4, and a strong negative correlation with Kiremt SPI4 and SPEI4. Therefore, the dryness and wetness situations in the basin are more significantly associated with ENSO(Nino3.4). From the temporal plot of the annual and June to September (Kiremt) season, the statistically significant correlations between SPI/SPEI and Nino3.4 index are about negative 0.45 to negative 0.61 over the basin. This shows a drought occurrence increase in the basin. The short rainy season (Belg) of the basin has a reasonable positive correlation of 0.35 to o.36 that reveals under the El Nino phase (Nino3.4), there might be an increase in wetness events over the basin. In addition, the annual and Kiremt season has a positive (0.31 to 0.53) SOI, which indicates that under SOI, there might be an increase in wetness conditions for the area during the last 34 years.
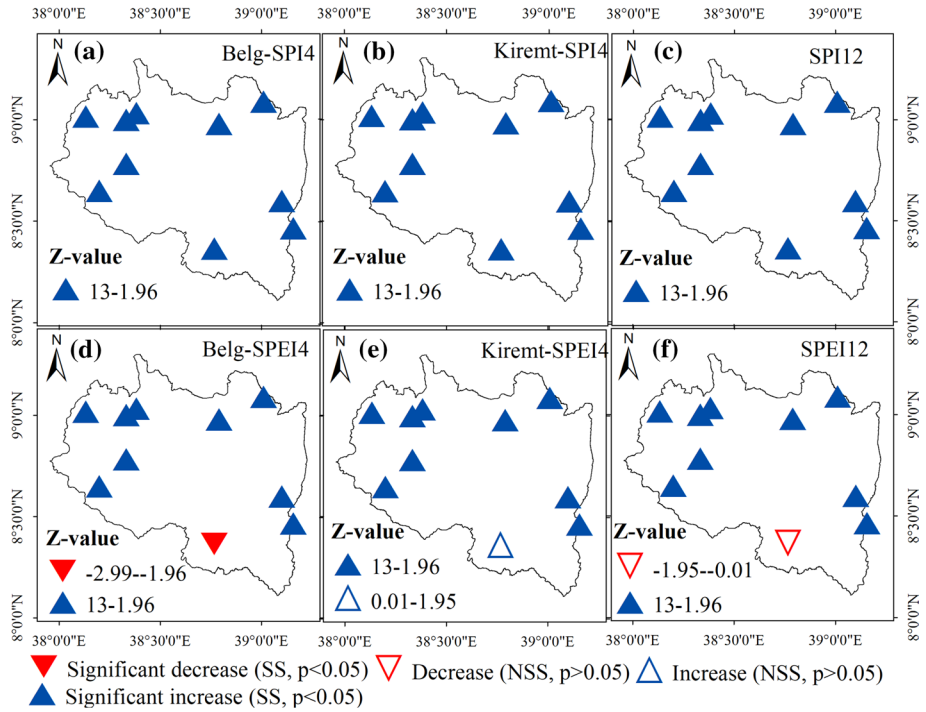
Fig. 7 Future seasonal drought trend of SPI and SPEI for RCP8.5 during 2020–2100
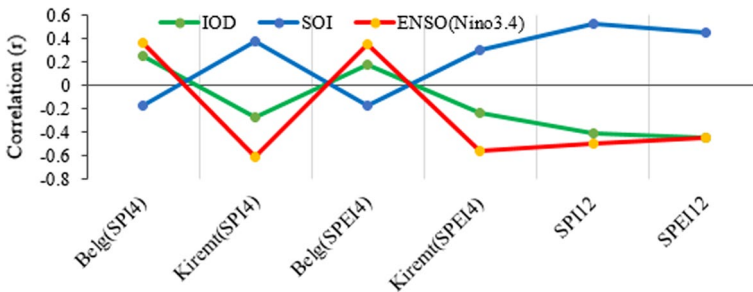
Fig. 8 Links between seasonal and annual drought indices (SPI/SPEI) with global climate indices (IOD, SOI, and ENSO (Nino3.4))

4 Discussion

In this paper, the SPI and SPEI at 4- and 12-months timescales were calculated using 34 (1983–2016) and 81 (2020–2100) year-long series of rainfall, minimum and maximum temperatures over ten stations in the UAB. The analysis includes temporal (Fig. 2e, Tables 3 and 4), spatial (Figs. 2 and 3) drought events for the past, and temporal (Fig. 4e and 5e, Tables 6, 7 and 8), spatial (Figs. 4, 5, 6 and 7) for the future of the Basin. This study found that the SDSM reproduces temperature better than rainfall (Table 2), and

the result is consistent with the findings of (Hassan et al., 2014). Rainfall was also more overestimated during calibration and underestimated during validation than temperature.

Overall, for the 4-month analysis, dry events were dominant for both the two indices (SPI 4 and SPEI4). This study identified some of the known major drought events for SPI and SPEI at 4-month timescales and showed dominant drought years in 1984, 1987, and 2015. These years coincided with Ethiopia's severe and extreme droughts observed by Gebreyesus (2020) and Mekonen et al. (2020). For the long time analysis, the SPI and SPEI were able to identify the years 1984, 1987, 1988, 2002, 2015, and 2016 as some of the major drought years in the study area (Fig. 2e). A consequence of this is the probability that longer timescales are well appropriate for detecting historically significant events, whereas shorter timescales display numerous seasonal and inter-annual variations (Degefu & Bewket, 2015; Mekonen et al., 2020). From this study, drought events of 4-month timescales happened more frequently but were of shorter duration than drought events of 12-month timescale. This finding is in agreement with Łabędzki (2007), Degefu and Bewket (2015), and Mekonen et al. (2020). Łabędzki (2007) also observed similar results in different parts of Ethiopia and the world.

The temporal evolution of the two drought indices (SPI and SPEI) for the short-time analysis indicates more moderate to extreme drought occurrences in the basin at the end of the twentieth century and the start of the twenty-first century (Fig. 2e). For the case of long-term analysis, which occurred less frequently, extreme droughts occurred in 1984, 2015, and 2016 by SPI and SPEI -12. Extreme drought showed a more rapid increment in the basin than severe and moderate droughts. The short-time analysis confirmed that drought years in the basin in the last 34 years happened in 1984, 1987, 2001, 2008–2009, and 2015 and 1984, 1987, 2015–2016 for SPI4 and SPEI4, respectively. This finding is similar to the report of Ghebrezgabher et al. (2016) that over 10 million people suffered from a food shortage due to drought in Ethiopia in 2015.

The impact of drought depends on the severity, duration, and spatial extent (Funk et al., 2008). In both SPI/SPEI for the 4- and 12-month time series, the most prolonged severe duration of drought events was displayed from 2002 to 2016 in spatial and temporal analysis. Generally, the result shows that the extended drought duration and magnitude of drought events were noted in the western parts and decreased in the eastern parts of the basin. The observed drying trend in the UAB over the study area could have been as of variations in the tropical Indo-Pacific SST (Liebmann et al., 2014; Williams & Funk, 2011). The large-scale atmospheric circulation variations linked with a weaker West African monsoon may have contributed to the long-term drought occurrence (Hua et al., 2018; Lyon & Dewitt, 2012). Every 2.5 years on average occurred in the past 34 years in the basin for a short period and 5 for the long-term 12-month analysis.

Even though SPEI is one of the robust indices in evaluating dryness and wetness (Ayugi et al., 2020; Ghebrezgabher et al., 2016; Polong et al., 2019), in this study, SPI also captured the wetness and dryness events almost similar to SPEI. However, as SPEI considers calculating drought PET, it is good to use for drought characterization. These results are reliable to data found in East Africa and the Horn, which showed an increase in SPEI during severe and extreme dry events (Mekasha et al., 2014). The extreme dry events may be related to the cycles of the El Niño-Southern Oscillation (ENSO) phenomenon (Rojas, 2020). During the Kiremt (JJAS) season in SPI, only three stations (Addis Alem, Koka Dam, and Mojo) showed a significant decrease in dry events. The annual trend of SPI showed a significant decrease in Addis Alem and Koka Dam, whereas in Addis Alem station significant decrease in the drying trend was observed in the SPEI drought index (Fig. 5). The annual drought trend test for SPI12 and SPEI12

showed an increasing trend of drought events except in the eastern and some parts of the northern basin. The increasing tendency of the annual drought was more significant in SPEI than SPI SPEI12 shows a significant drought trend in Ginchi and Hombole stations.

The finding from the seasonal analysis indicates that the main rainy (crop) season JJAS (Kiremt) of the basin revealed a mixing trend, whereas, in the short rainy season, FMAM (Belg) of the basin showed increasing dryness events. Based on the report of Mohammed et al. (2020), increasing drought frequencies in several parts of the world are mostly associated with the lack of air temperature rise, precipitation, and atmospheric evapotranspiration demand. Therefore, this increase in an annual drought causes water stress for the basin's crop production, hydropower production, domestic water supply, and irrigation activities. Based on the report of Mohammed et al. (2020), increasing drought frequencies in several parts of the world are mostly associated with the lack of air temperature rise, precipitation, and atmospheric evapotranspiration demand. Therefore, this increase in an annual drought causes water stress for the basin's crop production, hydropower production, domestic water supply, and irrigation activities. In this case, our result is similar to Haile et al. (2022), who found an overall increasing trend of drought from 1981 to 2016 in the Rift Valley sub-basin using the SPEI drought index. Therefore, it is likely that such relations exist with works with similar agro-ecological areas in East Africa, as Okal et al. (2020) found dryness trends increase in most of the area. Increased dryness in some parts of the basin during Kiremt has severe consequences on the production of sorghum, corn, and other crops in the basin (Temam et al., 2019). This implies agricultural production in the area will be affected.

The SPI and SPEI at 4- and 12-month timescales were simulated using SDSM on the RCP8.5 and RCP 4.5 scenarios from 2020 to 2100 over ten stations. The increasing dry events for the short and long term from 2020 to 2040 dominant for SPI and SPEI for the RCP4.5 indicates that the number of drought years increased dramatically at the UAB watershed (Table 6). This result agrees with Ayugi et al. (2021) who found that in the highland and lake regions of East Africa, there will likely be a decrease in drought occurrences in the future. The wetness will be observed from 2080 to 2100, whereas mixed dry and wet events experienced for around 20 years needs attention, as the basin is crucial for cropping and water resources. The common years during which more attention will be paid will be 2024, 2029, 2050, and 2051. The wetness of the predicted basin from 2080 to 2100 may be because of the prediction of an increment of likely extreme rainfall events in East Africa (Ongoma et al., 2018).

For the case of the highest scenario (RCP8.5), the drought will be severely and extremely high between 2020 and 2040 for SPI and SPEI (Fig. 5). Okafor et al. (2021) using the ensemble mean of the RCMs and considering RCPs 4.5 and 8.5 scenarios reported similar trends in which there will be a decrease in precipitation and significant warming from 2020 to 2049 in the Daso catchment of Burkina Faso. The highest drought was displayed by RCP8.5 than RCP4.5. Wet years will be observed from 2071 to 2100. As the report of Ongoma et al. (2018) reported, almost all of East Africa will experience a positive change in rainfall, and the increase will be higher under the RCP8.5 scenario than under the RCP4.5 scenario. In this research in both RCP4.5 and 8.5, the SPEI has shown slightly more drought conditions in the future compared to the SPI, which indicates an increase in PET compared to rainfall. This finding is broadly consistent with the findings of Nguvava et al. (2019) and Haile et al. (2020), which found similar results in East Africa. These results differ from others (e.g., Ahmadalipour et al. (2017) and Feng et al. (2017)), even though they also used SPI and SPEI. This may be due to the quality of data used in

this study, which is considered due to high resolution and combined/hybrid of station and satellite data.

In this study, the SPI and SPEI showed serious drought in the UAB from 1983 to 2016. For the case of the next 2020–2100 periods decreasing seasonal drought, a trend is displayed, but the drought in the basin is very serious in the future from 2020 to 2060. Generally, the risk of climate change because of its unpredictable variations in the future requires adapting food systems from climate change will require attention to more than just agricultural production, and needs adaptation and mitigation actions for efficient management of climate change influences on food security requires investment at present (el Mokhtar et al., 2019). Based on the evaluation of two drought indices for Kiremt and annual, future trends for SPEI_RCP4.5 showed a significant decrease in droughts except for Hombole station. For the Belg season, most climate stations displayed a non-significant trend for both SPI and SPEI except Koka Dam and Sendafa for SPI and Tulu Bolo for SPEI, which exhibited a significant decrease in dryness trends. However, the highest scenario, RCP8.5, indicates for both SPI and SPEI a significant decreasing trend of dryness events in the future in all three (Kiremt, Belg, and annual). Other studies in the basin have not previously indicated such a result. The present study raises the possibility that in the future, wetness will increase and severe droughts will decrease. These results are in harmony with recent studies showing that East Africa will show a wetter climate with more intense wet seasons and less severe droughts (Cook et al., 2020; Shongwe et al., 2011) Moreover, Spinoni et al. (2020) also found an expected significant rainfall increase in East Africa over the following few decades in answer to increased greenhouse gases.

4.1 Link of seasonal (SPI4/SPEI4) and annual (SPI/SPEI12) drought indices with the global climate indices

The temporal correlation of seasonal and annual with Nino3.4 and SOI indicates that SPI and SPEI over UAB correlate with ENSO (Nino3.4) and SOI. The variability of Belg and Kiremet season droughts in the UAB correlated with global climate indices, such as SOI and ENSO (Nino3.4). This finding agrees with the Woldegebrael et al.'s (2020) report that the Nino3.4 events are associated with the Belg and the main crop season Kiremt in Ethiopia. The association between Nino3.4 and SOI years can be useful for early warning in the main crop season (Kiremt).

4.2 Possible drivers, implications, and mitigation strategies for future drought hazards

Analyzing the historical drought and understanding projected spatiotemporal change in future drought patterns in UAB is crucial for policymakers and stakeholders to take mitigation measures earlier. The projected drought hazards affect the rainfed agricultural, socioeconomic activities, and water resources of society and the environment. Detecting the past and future projected drought in terms of duration, frequency, severity, intensity, and drought causes helps design a mitigation strategy. The projected future drought risks due to future climate change would cause regional to global terrestrial lands damages like East Africa and particularly UAB, and from time to time, it is seriously challenging rainfed agriculture and water resources under the existing increase in the greenhouse gas concentrations and warming of the climate system. Thus, prevention measures that should be taken in terms of different early warning systems and facilities derived from policies and

strategies for the policymakers like minimizing man-made effects and rehabilitation action to protect from environmental degradation may be some of them. Even though the magnitude/severity, duration, and frequency of drought in the area spatially are different, the observed impact of drought was will happen in Ethiopia in the near future, particularly in UAB.

To prevent the future risk of drought, different mitigation measures, like better water resources management strategies, building a drought-resilient economy, and inclusive implementation of environmental rehabilitation approaches, are some of the crucial (Gebrechorkos et al., 2019; Haile et al., 2020; Sheffield et al., 2014). As the basin is important for rainfed agriculture, water supplies for urban, industries, and irrigation thus, better preparedness for the future sustainable drought strategy and approaches by considering both local and global drivers are applied through designing policy with the advice of stakeholders. In addition, adaptation and mitigation priorities, strategies for water recycling, and community infrastructures in the UAB and other parts of the country especially the highland area of Ethiopia are vital.

5 Conclusion

The current study found that in the UAB, there was increased seasonal and annual dryness from 1983 to 2016. The research has shown that the drought event, duration, frequency, severity, and intensity in most climate stations have increased spatial drought change patterns during the same year. The droughts were mostly moderate to severe, with very few extreme cases. Droughts that lasted 4 months were more frequently observed than those that lasted 12 months. In the analysis, SPI mostly underestimated drought compared to SPEI, which better represented both severe and extreme droughts. Even though SPI and SPEI could capture the evolution of drought in identical years, there were also times when SPEI made a significant difference from SPI while displaying extreme and severe droughts. This indicates the necessity to use both or SPEI instead of SPI when either one is used alone. Based on the future evolution in the two (RCP4.5 and RCP8.5) scenarios, the dryness condition will continue at least shortly up to the 2030s and mid-2040s as far as extreme severe dryness is concerned, respectively. However, in the future projection of the seasonal and annual analyses, dry events will decrease from 2050 onwards. Future projection by RCP4.5 and RCP8.5, especially concerning the 12-month drought, indicates more droughts in the north and eastern part of the basin than in the rest. The projection of the 4-month drought will also be more frequent but milder than the drought that lasts twelve months. Out of the two scenarios, the highest intensity and extended drought soon are captured by RCP8.5 than RCP4.5. The basin spatially experiences severe and extreme droughts in most areas in the near future and reduction start from 2040 and onward. Higher drought changes are likely to occur in western and northeastern, while the central part of the basin is expected to have lower drought changes during 2020–2040 in UAB.

In addition to the local driving forces that influence drought occurrences, the result of this study found that IOD, SOI, and ENSO (Nino3.4) have an impact in the area. The observed periodicity of dryness/wetness over the UAB agreed with the negative/positive phase of SOI/ ENSO (Nino3.4) during Belg and the positive/negative phase during Kiremt (SPI4/SPEI4). The evidence from this study suggests that classified drought projection in different future periods is key for minimizing and early coping of climate change impacts on drought-like 2020–2040, 2041–2060, and 2061–2100. The present study confirms some

previous findings in East Africa and contributes additional evidence that suggests developing basin-wide targeted interventions aimed at protecting livelihoods and the environment from drought hazards soon (2020–2040) that the agriculture and water resources would affect. However, at the end of the 21st-century, dryness would decrease and wetness increase. From this result, another extreme might happen like a flood, so more attention must also be given to the end of the twenty-first century as drought in the near future. Taken together, these findings are useful for better preparedness for the future sustainable drought strategy and applying adaptation and mitigation priorities, strategies for water recycling and rehabilitation, community infrastructures in the UAB and other parts of the country, especially the highland area of Ethiopia, as the basin is important for rainfed agricultural, water supplies for urban and industries and irrigation. The result, therefore, provides valuable evidence on local drought frequency, duration, magnitude/severity, intensity, trend, and the global driver's consequence on drought incidents in the UAB. The outcomes of this study can be used as a baseline for other basins with similar agro-ecological environments. Taken together, these findings are useful to better the future sustainable drought strategy development and apply adaptation and mitigation priorities that are aimed at protecting the society and the environment from drought hazards soon (2020–2060) that the agriculture and water resources would affect. It is suggested that more research be undertaken in the characterization of projected socioeconomic drought affected by climate change, risk management assessment, and changes in rainfall and temperature extremes. For future projection, the statistical downscaling method was used. So, one can try in the future using the dynamic downscaling method for comparison purposes.

Availability of data Additional data will available upon request.

Declarations

Conflict of interest The authors declare that there is no conflict of interest regarding the publication of this paper.

References

Adane, G. B., Hirpa, B. A., Lim, C. H., & Lee, W. K. (2020). Spatial and temporal analysis of dry and wet spells in upper awash river basin, ethiopia. *Water*. https://doi.org/10.3390/w12113051

Ahmadalipour, A., Moradkhani, H., & Demirel, M. C. (2017). A comparative assessment of projected meteorological and hydrological droughts: elucidating the role of temperature. *Civil and Environmental Engineering Faculty Publications and Presentations*. https://doi.org/10.1016/j.jhydrol.2017.08.047

Ahmed, K., Shahid, S., Harun, S. B., & Wang, X. (2016). Characterization of seasonal droughts in Balochistan Province, Pakistan. *Stochastic Environmental Research and Risk Assessment, 30*(2), 747–762. https://doi.org/10.1007/s00477-015-1117-2

Allen, R. G., Pereira, L. S., Raes, D., & Smith, M. (1998). *Crop evapotranspiration-Guidelines for computing crop water requirements-FAO Irrigation and drainage paper 56*.

Ayugi, B., Shilenje, Z. W., Lim, K. T. C., Sian, K., Mumo, R., Dike, V. N., Chehbouni, A., & Ongoma, V. (2021). *Projected Changes in Meteorological Drought Over East Africa Inferred from Bias-Adjusted CMIP6 Models*. https://doi.org/10.21203/rs.3.rs-983012/v1

Ayugi, B., Tan, G., Rouyun, N., Zeyao, D., Ojara, M., Mumo, L., Babaousmail, H., & Ongoma, V. (2020). Evaluation of meteorological drought and flood scenarios over Kenya, East Africa. *Atmosphere*. https://doi.org/10.3390/atmos11030307

Azazh, B. (2008). *Water Allocation Study of Upper Awash Valley for Existing and Future Demands (from Koka Reservoir to Metehara Area)*. Addis Ababa.

Beguería, S., Vicente-Serrano, S. M., Reig, F., & Latorre, B. (2014). Standardized precipitation evapotranspiration index (SPEI) revisited: Parameter fitting, evapotranspiration models, tools, datasets and drought monitoring. *International Journal of Climatology, 34*(10), 3001–3023. https://doi.org/10.1002/joc.3887

Belayneh, A., Adamowski, J., & Khalil, B. (2016). Short-term SPI drought forecasting in the Awash River Basin in Ethiopia using wavelet transforms and machine learning methods. *Sustainable Water Resources Management, 2*(1), 87–101. https://doi.org/10.1007/s40899-015-0040-5

Below, R., Grover-Kopec, E., & Dilley, M. (2007). Documenting drought-related Disasters: A global reassessment. *Journal of Environment and Development, 16*(3), 328–344. https://doi.org/10.1177/1070496507306222

Bezu, A. (2020). Analyzing impacts of climate variability and changes in Ethiopia: A review. *American Journal of Modern Energy, 6*(3), 65. https://doi.org/10.11648/j.ajme.20200603.11

Bhaga, T. D., Dube, T., Shekede, M. D., & Shoko, C. (2020). Impacts of climate variability and drought on surface water resources in sub-saharan africa using remote sensing: A review. *Remote Sensing., 12*(24), 1–34. https://doi.org/10.3390/rs12244184

Bobrowsky, P. T. (2013). *Encyclopedia of Natural Hazards*. In P. T. Bobrowsky (Ed.). Springer: Netherlands. https://doi.org/10.1007/978-1-4020-4399-4

Burnett, D. (2013). Stage 2-supporting climate resilient value chains. *UK Department for International Development (DFID)*. https://doi.org/10.12774/eod_cr.april2015.burnettd

Cook, K. H., Fitzpatrick, R. G. J., Liu, W., & Vizy, E. K. (2020). Seasonal asymmetry of equatorial East African rainfall projections: Understanding differences between the response of the long rains and the short rains to increased greenhouse gases. *Climate Dynamics, 55*(7–8), 1759–1777. https://doi.org/10.1007/s00382-020-05350-y

Dai, A. (2011). Drought under global warming: A review. In *Wiley Interdisciplinary Reviews: Climate Change* (Vol. 2, Issue 1, pp. 45–65). Wiley-Blackwell. https://doi.org/10.1002/wcc.81

Degefu, M. A., & Bewket, W. (2015). Trends and spatial patterns of drought incidence in the Omo-Ghibe River Basin, Ethiopia. *Geografiska Annaler, Series a: Physical Geography, 97*(2), 395–414. https://doi.org/10.1111/geoa.12080

Dinku T, Hansen J, Rose A, Damen B, S. M. (2018). Enhancing national climate services (ENACTS) approach to support climate resilience in agriculture. In *CCAFS Info Note. Wageningen, Netherlands: CGIAR Research Program on Climate Change, Agriculture and Food Security (CCAFS)*. (Issue December).

Dinku, T., Block, P., Sharoff, J., Hailemariam, K., Osgood, D., del Corral, J., Cousin, R., & Thomson, M. C. (2014). Bridging critical gaps in climate services and applications in africa. *Earth Perspectives, 1*(1), 15. https://doi.org/10.1186/2194-6434-1-15

Dubache, G., Ogwang, B. A., Ongoma, V., & Towfiqul Islam, A. R. M. (2019). The effect of Indian Ocean on Ethiopian seasonal rainfall. *Meteorology and Atmospheric Physics, 131*(6), 1753–1761. https://doi.org/10.1007/s00703-019-00667-8

Esayas, B., Simane, B., Teferi, E., Ongoma, V., & Tefera, N. (2018). Trends in extreme climate events over three agroecological zones of Southern Ethiopia. *Advances in Meteorology*. https://doi.org/10.1155/2018/7354157

Fanadzo, M., Ncube, B., French, A., & Belete, A. (2021). Smallholder farmer coping and adaptation strategies during the 2015–18 drought in the Western Cape, South Africa. *Physics and Chemistry of the Earth*. https://doi.org/10.1016/j.pce.2021.102986

Farooqi, Z. U. R., Zia Ur Rehman, M., Sohail, M. I., Usman, M., Khalid, H., & Naz, K. (2020). Regulation of drought stress in plants. In *Plant Life under Changing Environment: Responses and Management* (pp. 77–104). Elsevier. https://doi.org/10.1016/B978-0-12-818204-8.00004-7

Feng, S., Trnka, M., Hayes, M., & Zhang, Y. (2017). Why do different drought indices show distinct future drought risk outcomes in the U.S. Great Plains? *Journal of Climate, 30*(1), 265–278. https://doi.org/10.1175/JCLI-D-15-0590.1

Funk, C. C. (2012). Exceptional warming in the western Pacific-Indian Ocean warm pool has contributed to more frequent droughts in eastern Africa. *Bulletin of the American Meteorological Society, 93*, 1049–1051.

Funk, C., Dettinger, M. D., Michaelson, J., Verdin, J., & Brown, M. E. (2008). The warm ocean dry Africa dipole controls decadal moisture transports threatening food insecure Africa. *Proceedings of the National Academy of Sciences, 105*, 11081–11086.

Gautam, M. (2006). Managing Drought in Sub-Saharan Africa: Policy Perspectives 1. *Economic Consequences and Policies for Mitigation, at the IAAE Conference, Gold Coast, Queensland, Australia, August 12–18*, 1–18. www.em-dat.net

Gebrechorkos, S. H., Hülsmann, S., & Bernhofer, C. (2019). Regional climate projections for impact assessment studies in East Africa. *Environmental Research Letters*. https://doi.org/10.1088/1748-9326/ab055a

Gebremichael, H. B., Raba, G. A., Beketie, K. T., Feyisa, G. L., & Siyoum, T. (2022). Changes in daily rainfall and temperature extremes of upper Awash Basin Ethiopia. *Scientific African*. https://doi.org/10.1016/j.sciaf.2022.e01173

Gebreyesus, M. (2020). Historical drought characterization in Awash River Basin, Ethiopia. *International Journal of Environmental Sciences & Natural Resources., 26*(3), 70–77. https://doi.org/10.19080/ijesnr.2020.26.556186

Getaneh, Y., Alemu, A., Ganewo, Z., & Haile, A. (2022). Food security status and determinants in North-Eastern rift valley of Ethiopia. *Journal of Agriculture and Food Research*. https://doi.org/10.1016/j.jafr.2022.100290

Gezie, M. (2019). Farmer's response to climate change and variability in Ethiopia: A review. In *Cogent Food and Agriculture* (Vol. 5, Issue 1). Informa Healthcare. https://doi.org/10.1080/23311932.2019.1613770

Ghebrezgabher, M. G., Yang, T., & Yang, X. (2016). Long-term trend of climate change and drought assessment in the Horn of Africa. *Advances in Meteorology*. https://doi.org/10.1155/2016/8057641

Gupta, H. V., Kling, H., Yilmaz, K. K., & Martinez, G. F. (2009). Decomposition of the mean squared error and NSE performance criteria: Implications for improving hydrological modelling. *Journal of Hydrology, 377*(1–2), 80–91. https://doi.org/10.1016/j.jhydrol.2009.08.003

Haile, B. T., Bekitie, K. T., Zeleke, T. T., Ayal, D. Y., Feyisa, G. L., & Anose, F. A. (2022). Drought analysis using standardized evapotranspiration and aridity index at bilate watershed: Sub-Basins of Ethiopian Rift Valley. *The Scientific World Journal*. https://doi.org/10.1155/2022/1181198

Haile, G. G., Tang, Q., Hosseini-Moghari, S. M., Liu, X., Gebremicael, T. G., Leng, G., Kebede, A., Xu, X., & Yun, X. (2020). Projected impacts of climate change on drought patterns over East Africa. *Earth's Future*. https://doi.org/10.1029/2020EF001502

Halcrow. (2006). Awash River Basin flood control and watershed management study project. Working Paper 2. Review and assessment of community development, settlement patterns and gender in the Awash River Basin (pp 46).

Hamed, K. H., & Rao, A. R. (1998). Hydrology A modified Mann-Kendall trend test for autocorrelated data. *Journal of Hydrology, 204*(1–4), 182–196.

Hao, Z., & Singh, V. P. (2015). Drought characterization from a multivariate perspective: A review. *Journal of Hydrology, 527*, 668–678.

Hargreaves, G. H., Asce, F., & Allen, R. G. (2003). History and evaluation of Hargreaves evapotranspiration equation. *Journal of Irrigation and Drainage Engineering*. https://doi.org/10.1061/ASCE0733-94372003129:153

Hassan, Z., Shamsudin, S., & Harun, S. (2014). Application of SDSM and LARS-WG for simulating and downscaling of rainfall and temperature. *Theoretical and Applied Climatology, 116*(1–2), 243–257. https://doi.org/10.1007/s00704-013-0951-8

Ho, C. K., Stephenson, D. B., Collins, M., Ferro, C. A. T., & Brown, S. J. (2012). Calibration strategies a source of additional uncertainty in climate change projections. *Bulletin of the American Meteorological Society, 93*(1), 21–26. https://doi.org/10.1175/2011BAMS3110.1

Hua, W., Zhou, L., Chen, H., Nicholson, S. E., Jiang, Y., & Raghavendra, A. (2018). Understanding the Central Equatorial African long-term drought using AMIP-type simulations. *Climate Dynamics, 50*(3–4), 1115–1128. https://doi.org/10.1007/s00382-017-3665-2

Kalnay, E., Kanamitsu, M., Kistler, R., Collins, W., Deaven, D., et al. (1996). The NCEP/NCAR 40-year reanalysis project. *Bulletin of the American Meteorological Society, 77*(3), 437–472.

Kaushal, M. (2019). Portraying rhizobacterial mechanisms in drought tolerance. In *PGPR Amelioration in Sustainable Agriculture* (pp. 195–216). Elsevier. https://doi.org/10.1016/b978-0-12-815879-1. 00010-0.

Kerim, T., Abebe, A., Hussen, B., Engineering, I., Minch, A., & Minch, A. (2016). Study of water allocation for existing and future demands under changing climate condition: Case of upper Awash Sub River Basin. *Journal of Environment and Earth Science, 6*(10), 18–31.

Kurkura M. (2011). *Water Balance of Upper Awash Basin Based on Satellite-Derived Data (Remote Sensing)*. Addis Ababa University.

Łabędzki, L. (2007). Estimation of local drought frequency in central Poland using the standardized precipitation index SPI. *Irrigation and Drainage, 56*(1), 67–77. https://doi.org/10.1002/ird.285

Liebmann, B., Hoerling, M. P., Funk, C., Bladé, I., Dole, R. M., Allured, D., Quan, X., Pegion, P., & Eischeid, J. K. (2014). Understanding recent eastern Horn of Africa rainfall variability and change. *Journal of Climate, 27*(23), 8630–8645. https://doi.org/10.1175/JCLI-D-13-00714.1

Lyon, B., & Dewitt, D. G. (2012). A recent and abrupt decline in the East African long rains. *Geophysical Research Letters*. https://doi.org/10.1029/2011GL050337

Mbiriri, M., Mukwada, G., & Manatsa, D. (2019). Spatiotemporal characteristics of severe dry and wet conditions in the Free State Province South Africa. *Theoretical and Applied Climatology, 135*(1–2), 693–706. https://doi.org/10.1007/s00704-018-2381-0

Mckee, T. B., Doesken, N. J., & Kleist, J. (1993). The relationship of drought frequency and duration to time scales. In *Eighth Conference on Applied Climatology*.

Mekasha, A., Tesfaye, K., & Duncan, A. J. (2014). Trends in daily observed temperature and precipitation extremes over three Ethiopian eco-environments. *International Journal of Climatology, 34*(6), 1990–1999. https://doi.org/10.1002/joc.3816

Mekonen, A. A., Berlie, A. B., & Ferede, M. B. (2020). Spatial and temporal drought incidence analysis in the northeastern highlands of Ethiopia. *Geoenvironmental Disasters*. https://doi.org/10.1186/s40677-020-0146-4

Meza, I., Eyshi Rezaei, E., Siebert, S., Ghazaryan, G., Nouri, H., Dubovyk, O., Gerdener, H., Herbert, C., Kusche, J., Popat, E., Rhyner, J., Jordaan, A., Walz, Y., & Hagenlocher, M. (2021). Drought risk for agricultural systems in South Africa: Drivers, spatial patterns, and implications for drought risk management. *Science of the Total Environment*. https://doi.org/10.1016/j.scitotenv.2021.149505

Mohammed, S., Alsafadi, K., Al-Awadhi, T., Sherief, Y., Harsanyie, E., & el Kenawy, A. M. (2020). Space and time variability of meteorological drought in Syria. *Acta Geophysica, 68*(6), 1877–1898. https://doi.org/10.1007/s11600-020-00501-5

Mokhtar, M. A., Anli, M., ben Laouane, R., Boutasknit, A., Boutaj, H., Draoui, A., Zarik, L., & Fakhech, A. (2019). Food security and climate change. In *IGI Global* (pp. 53–73). https://doi.org/10.4018/978-1-5225-7775-1.ch004

Moriasi, D. N., Arnold, J. G., Liew, M. W. van, Bingner, R. L., Harmel, R. D., & Veith, T. L. (1983). Model evaluation guidelines for systematic quantification of accuracy in watershed simulations. In *Transactions of the ASABE* (Vol. 50, Issue 3).

Nash, E. I., & SutCLIFFF, J. V. (1970). River flow forecasting through conceptual model part I- A discussion of principle. *Jornal of Hydrology, 10*, 282–290.

Nguvava, M., Abiodun, B. J., & Otieno, F. (2019). Projecting drought characteristics over East African basins at specific global warming levels. *Atmospheric Research, 228*, 41–54. https://doi.org/10.1016/j.atmosres.2019.05.008.

Okafor, G. C., Larbi, I., Chukwuma, E. C., Nyamekye, C., Limantol, A. M., & Dotse, S. Q. (2021). Local climate change signals and changes in climate extremes in a typical Sahel catchment: The case of Dano catchment, Burkina Faso. *Environmental Challenges*. https://doi.org/10.1016/j.envc.2021.100285

Okal, H. A., Ngetich, F. K., & Okeyo, J. M. (2020). Spatio-temporal characterisation of droughts using selected indices in Upper Tana River watershed, Kenya. *Scientific African*. https://doi.org/10.1016/j.sciaf.2020.e00275

Ongoma, V., Chena, H., & Gaoa, C. (2018). Projected changes in mean rainfall and temperature over east Africa based on CMIP5 models. *International Journal of Climatology, 38*(3), 1375–1392. https://doi.org/10.1002/joc.5252

Park, S., Im, J., Park, S., & Rhee, J. (2017). Drought monitoring using high resolution soil moisture through multi-sensor satellite data fusion over the Korean peninsula. *Agricultural and Forest Meteorology, 237–238*, 257–269. https://doi.org/10.1016/j.agrformet.2017.02.022

Patakamuri, S. K. (2021). *Package "modifiedmk" Title Modified Versions of Mann Kendall and Spearman's Rho Trend Tests*. https://doi.org/10.1017/CBO9781107415324.004

Patakamuri, S. K., Muthiah, K., & Sridhar, V. (2020). Long-Term homogeneity, trend, and change-point analysis of rainfall in the arid district of ananthapuramu, Andhra Pradesh State, India. *Water*. https://doi.org/10.3390/w12010211

Peña-Guerrero, M. D., Nauditt, A., Muñoz-Robles, C., Ribbe, L., & Meza, F. (2020). Drought impacts on water quality and potential implications for agricultural production in the Maipo River Basin, Central Chile. *Hydrological Sciences Journal, 65*(6), 1005–1021. https://doi.org/10.1080/02626667.2020.1711911

Polong, F., Chen, H., Sun, S., & Ongoma, V. (2019). Temporal and spatial evolution of the standard precipitation evapotranspiration index (SPEI) in the Tana River Basin, Kenya. *Theoretical and Applied Climatology, 138*(1–2), 777–792. https://doi.org/10.1007/s00704-019-02858-0

Report, W. M. O. (2006). *Drought monitoring and early warning: concepts, progress and future challenges*. World Meteorological Organization.

Rojas, O. (2020). Agricultural extreme drought assessment at global level using the FAO-agricultural stress index system (ASIS). *Weather and Climate Extremes*. https://doi.org/10.1016/j.wace.2018.09.001

Senamaw, A., Addisu, S., & Suryabhagavan, K. V. (2021). Mapping the spatial and temporal variation of agricultural and meteorological drought using geospatial techniques Ethiopia. *Environmental Systems Research*. https://doi.org/10.1186/s40068-020-00204-2

Sheffield, J., Wood, E. F., Chaney, N., Guan, K., Sadri, S., Yuan, X., Olang, L., Amani, A., Ali, A., Demuth, S., & Ogallo, L. (2014). A drought monitoring and forecasting system for sub-sahara african water resources and food security. *Bulletin of the American Meteorological Society, 95*(6), 861–882. https://doi.org/10.1175/BAMS-D-12-00124.1

Shekhar, A., & Shapiro, C. A. (2019). What do meteorological indices tell us about a long-term tillage study? *Soil & Tillage Research, 193*, 161–170. https://doi.org/10.1016/j.still.2019.06.004.

Shepherd, A., Mitchell, T., Lewis, K., Lenhardt, A., Jones, L., Scott, L., & Muir-Wood, R. (2013). *The geography of poverty, disasters and climate extremes in 2030*. ODI London.

Shi, B., & Hussain, S. S. (2020). Toward elucidating the functions of miRNAs in drought stress tolerance. In *Plant Small RNA* (pp. 231–246). Elsevier. https://doi.org/10.1016/b978-0-12-817112-7.00012-2

Shiferaw, B., Tesfaye, K., Kassie, M., Abate, T., Prasanna, B. M., & Menkir, A. (2014). Managing vulnerability to drought and enhancing livelihood resilience in sub-Saharan Africa: Technological, institutional and policy options. *Weather and Climate Extremes, 3*, 67–79. https://doi.org/10.1016/j.wace.2014.04.004

Shongwe, M. E., van Oldenborgh, G. J., van den Hurk, B., & van Aalst, M. (2011). Projected changes in mean and extreme precipitation in Africa under global warming. Part II: East Africa. *Journal of Climate, 24*(14), 3718–3733.

Slette, I. J, Post, A. K., Awad, M, et al. (2019). How ecologists define drought, and why we should do better. *Global Change Biology, 25*, 3193–3200. https://doi.org/10.1111/gcb.14747.

Spinoni, J., Barbosa, P., Bucchignani, E., Cassano, J., Cavazos, T., Christensen, J. H., Christensen, O. B., Coppola, E., Evans, J., Geyer, B., Giorgi, F., Hadjinicolaou, P., Jacob, D., Katzfey, J., Koenigk, T., Laprise, R., Lennard, C. J., Kurnaz, M. L., Delei, L. I., & Dosio, A. (2020). Future global meteorological drought hot spots: A study based on CORDEX data. *Journal of Climate, 33*(9), 3635–3661. https://doi.org/10.1175/JCLI-D-19-0084.1

Srinivasarao, C., Rao, K. V., Gopinath, K. A., Prasad, Y. G., Arunachalam, A., Ramana, D. B. V., Chary, G. R., Gangaiah, B., Venkateswarlu, B., & Mohapatra, T. (2020). Agriculture contingency plans for managing weather aberrations and extreme climatic events: Development, implementation and impacts in India. In *Advances in Agronomy* (vol. 159, pp. 35–91). Academic Press Inc. https://doi.org/10.1016/bs.agron.2019.08.002

Tadesse, T., Haile, M., Senay, G., Wardlow, B. D., & Knutson, C. L. (2008). The need for integration of drought monitoring tools for proactive food security management in sub-Saharan Africa. *Natural Resources Forum, 32*, 265–279.

Tate, E. L., & Gustard, A. (2000). Drought definition: a hydrological perspective. In *Drought and drought mitigation in Europe* (pp. 23–48). Springer: Dordrecht.

Temam, D., Uddameri, V., Mohammadi, G., Hernandez, E. A., & Ekwaro-Osire, S. (2019). Long-term drought trends in Ethiopia with implications for dryland agriculture. *Water*. https://doi.org/10.3390/w11122571

Trenberth, K. E., Dai, A., van der Schrier, G., Jones, P. D., Barichivich, J., Briffa, K. R., & Sheffield, J. (2014). Global warming and changes in drought. In *Nature Climate Change* (vol. 4, Issue 1, pp. 17–22). https://doi.org/10.1038/nclimate2067

Tsakiris, G., & Vangelis, H. (2005). Establishing a drought index incorporating evapotranspiration. *European Water, 9*(10), 4–11.

Vicente-Serrano, S. M., Beguería, S., & López-Moreno, J. I. (2010). A multiscalar drought index sensitive to global warming: The standardized precipitation evapotranspiration index. *Journal of Climate, 23*(7), 1696–1718. https://doi.org/10.1175/2009JCLI2909.1

Vicente-Serrano, S. M., Beguería, S., Lorenzo-Lacruz, J., Camarero, J. J., López-Moreno, J. I., Azorin-Molina, C., Revuelto, J., Morán-Tejeda, E., & Sanchez-Lorenzo, A. (2012). Performance of drought indices for ecological, agricultural, and hydrological applications. *Earth Interactions, 16*(10), 1–27.

Wang, X., Hou, X., Li, Z., & Wang, Y. (2014). Spatial and temporal characteristics of meteorological drought in Shandong Province, China, from 1961 to 2008. *Advances in Meteorology*. https://doi.org/10.1155/2014/873593

Wilby, R. L., Dawson, C. W., & Barrow, E. M. (2002). sdsm-a decision support tool for the assessment of regional climate change impacts. In *Environmental Modelling & Software* (vol. 17). www.elsevier.com/locate/envsoft

Wilby, R. L., & Dawson, C. W. (2007). SDSM 4.2-A decision support tool for the assessment of regional climate change impacts User Manual. In *UKSDSM*. http://www.cics.uvic.ca/scenarios/index.cgi?Scenarios

Wilby, R. L., & Dawson, C. W. (2015). *Statistical DownScaling Model-Decision Centric (SDSM-DC)*.

Wilhite, D. A. (2000). Chapter 1 Drought as a Natural Hazard: Concepts and Definitions CORE Metadata, citation and similar papers at core.ac.uk Provided by DigitalCommons@University of Nebraska. *Drought: A Global Assessment, 1*, 3–18. http://digitalcommons.unl.edu/droughtfacpub/69

Wilhite, D. A. (2003). Drought. In J. R. Holton (Ed.), *Encyclopedia of Atmospheric Sciences* (pp. 650–658). Academic Press. https://doi.org/10.1016/B0-12-227090-8/00037-3

Wilhite, D. A., & Glantz, M. H. (1985). Understanding: The Drought Phenomenon: The Role of Definitions. *Water International, 10*(3), 111–120. https://doi.org/10.1080/02508068508686328

Williams, A. P., & Funk, C. (2011). A westward extension of the warm pool leads to a westward extension of the Walker circulation, drying eastern Africa. *Climate Dynamics, 37*(11–12), 2417–2435. https://doi.org/10.1007/s00382-010-0984-y

Woldegebrael, S. M., Kidanewold, B. B., Zaitchik, B., & Melesse, A. M. (2020). Rainfall and flood event interrelationship - a case study of awash and Omo-Gibe Basins, Ethiopia. *International Journal of Scientific & Engineering Research, 11*(1), 332–343.

Workie, T. G., & Debella, H. J. (2018). Climate change and its effects on vegetation phenology across ecoregions of Ethiopia. *Global Ecology and Conservation*. https://doi.org/10.1016/j.gecco.2017.e00366

Yacoub, E., & Tayfur, G. (2020). Spatial and temporal of variation of meteorological drought and precipitation trend analysis over whole Mauritania. *Journal of African Earth Sciences*. https://doi.org/10.1016/j.jafrearsci.2020.103761

Yang, C., Tuo, Y., Ma, J., & Zhang, D. (2019). Spatial and temporal evolution characteristics of drought in Yunnan Province from 1969 to 2018 based on SPI/SPEI. *Water, Air, and Soil Pollution*. https://doi.org/10.1007/s11270-019-4287-6

Yao, N., Li, L., Feng, P., Feng, H., Li Liu, D., Liu, Y., Jiang, K., Hu, X., & Li, Y. (2020). Projections of drought characteristics in China based on a standardized precipitation and evapotranspiration index and multiple GCMs. *Science of the Total Environment*. https://doi.org/10.1016/j.scitotenv.2019.135245

Zambrano-Bigiarini, M. (2020). *Goodness-of-fit Measures to Compare Observed and Simulated Values with hydroGOF*.

Zambreski, Z. T., Professor, M., & Lin, X. (2016). *A statistical assessment of drought variability and climate prediction for Kansas*. Cornell University.

Zehtabian, Gh. R., Salajegheh, A., Malekian, A., Boroomand, N., & Azareh, A. (2016). Evaluation and comparison of performance of SDSM and CLIMGEN models in simulation of climatic variables in Qazvin plain. *Desert, 21*(2), 147–156.

Authors and Affiliations

Haftu Brhane Gebremichael[1] · **Gelana Amente Raba[1]** · **Kassahun Ture Beketie[2]** · **Gudina Legese Feyisa[2]**

Gelana Amente Raba
amentegelana@gmail.com

Kassahun Ture Beketie
tkassa2010@gmail.com

Gudina Legese Feyisa
fgudina@gmail.com

[1]   Department of Physics, College of Natural and Computational Sciences, Haramaya University, P.O. Box: 138, Dire Dawa, Ethiopia

[2]   Center of Environmental Sciences, College of Natural and Computational Sciences Addis Ababa University, P.O. Box: 1176, Addis Ababa, Ethiopia